

**ANTIMICROBIAL ACTIVITY OF SILK FIBROIN
MICROPARTICLES**

**A THESIS SUBMITTED TO
THE GRADUATE SCHOOL OF APPLIED SCIENCES
OF
NEAR EAST UNIVERSITY**

**By
CHIDI WILSON NWEKWO**

**In Partial Fulfilment of the Requirements for
the Degree of Master of Science
in
Biomedical Engineering**

NICOSIA, 2015

Chidi Wilson Nwekwo: Antimicrobial Activity of Silk Fibroin Microparticles

Approval of Director of Graduate School of Applied Sciences

Prof. Dr. İlkey SALİHOĞLU

Director

We certify this thesis is satisfactory for the award of the Degree of

Master of Science in Biomedical Engineering

Examining Committee In Charge:

Prof. Dr. Nedim Çakır	Committee Chairman, Department of Internal Medicine, NEU.
Assoc. Prof. Dr. Terin Adali	Supervisor, Department of Biomedical Engineering, NEU
Assoc. Prof. Dr. Kaya Süer	Co-Supervisor, Department of Clinical Microbiology and Infectious Diseases, NEU.
Assoc. Prof. Dr. Dudu Özkum Yavuz	Department of Pharmaceutical Botany, NEU.
Assist. Prof. Dr. Murat Uncu	Department of Clinical Biochemistry, NEU.

I hereby declare that the research work embodied in this dissertation on the “Antimicrobial Activity of Silk Fibroin Microparticles” is original and has not yet been submitted in part or in full for a degree to the best of our knowledge. In addition, I also declare that all the information contained in this document conforms to the academic rules and ethical standards, having cited and reference all materials that further solidify the originality of this work.

Name, Last Name: Chidi Wilson Nwekwo

Signature:

Date:

ACKNOWLEDGEMENT

Firstly, I would like to thank God Almighty for the wonderful privilege of having Our head of department, Assoc. Prof. Dr. Terin Adali as supervisor and Assoc. Prof. Dr. Kaya Süer, Department of Clinical Microbiology and Infectious Diseases as co-supervisor. Who were of tremendous help, even with their busy schedule mapped out time to see to the successful completion of this work.

I would also like to acknowledge Bio. Emrah Güler, Meryem Güvenir, and Ayse Arikan, who were of great assistance even with their own personal responsibilities still had room for me. They made me feel very much at home in their Laboratory.

Special thanks to my wonderful colleagues Emmanuel Olaolu, Deborah Francis, Vivian Okafor, Lucy Abijah, Lewis Guru, Coston Pwadi, and Fatih Veysel Nurcin in a shortlist for lack of space. Whose presence around even when they don't speak meant everything to me and work times were always fun times together.

My parents to whom every of this won't have happened if they had not entrusted me with this special privilege and I bless God for them. Not forgetting my younger ones Tochi, Alex, and Nonso, I won't trade them for anything in this World.

And finally again, I thank God Almighty so much for all I had and will ever need He faithfully provides. It has always been and will always be all about Him.

To God Almighty....

ABSTRACT

The cocoon of *Bombyx mori* silkworm is a very important biomaterial for biomedical applications. The main aim of this work is, the modification of their antimicrobial properties on interaction with six selected microbes namely *Escherichia coli* (ATCC 25922), *Candida albicans* (ATCC 90028), *Staphylococcus aureus* (ATCC 25923), *Enterococcus faecalis* (ATCC 29212), *Bacillus cereus* (ATCC 10876), and *Pseudomonas aeruginosa* (ATCC 27853). Silk fibroin derived from the cocoons of the silkworm, *Bombyx mori* was synthesized into microparticles by the use of an ionotropic gelation technique with sodium tripolyphosphate (TPP) as a cross-linking agent. The microparticles of diameter 1 to 1000 μm or microns were also loaded with two variant drugs belonging to the family of fluoroquinolones, Floxin and Cipro with active ingredients Ofloxacin and Ciprofloxacin respectively. Several ratios of the drugs were used in incorporation with the silk fibroin and characterization of particles were done by SEM, XRD, and antimicrobial analysis.

The samples exhibited remarkable antimicrobial activity against *Escherichia coli*, *Staphylococcus aureus*, *Enterococcus faecalis*, *Bacillus cereus*, and *Pseudomonas aeruginosa*, no antimicrobial activity was exhibited against *Candida albicans*. The benefit of using silk fibroin, which is the potent protein in silk, has been established in several biomedical applications. Silk fibroin microparticles also demonstrated high aerosolization performance. And also has a great potential of been used in wound healing to enhance drying and a sterile environment for the healing process.

Keywords: Silk Fibroin, Microparticles, Tripolyphosphate, Ionotropic Gelation, Antimicrobial activity

ÖZET

Bombyx Mori ipek böceğinden elde edilen kozalar, biyomedikal uygulamalar için çok önemlidir. Bu çalışmanın amacı, anti-mikrobiyal özelliğini geliştirmek amaçlı modifiye edilmiş ipek fibroin proteinini *Escherichia coli* (ATCC 25922), *Candida albicans* (ATCC 90028), *Staphylococcus aureus* (ATCC 25923), *Enterococcus faecalis* (ATCC 29212), *Bacillus cereus* (ATCC 10876), ve *Pseudomonas aeruginosa* (ATCC 27853) etkileşimini incelemektir. Sodyum tripolifosfat ile iyonotropik jelleşme tekniği kullanılarak ipek fibroin proteininden mikroküreler elde edildi. Florokuinolon familyasına ait ofloksasin ve siprofloksasin aktif maddelerini içeren Floxin ve Cipro ilaçları ile yüklenen küreler, 1 ile 1000 µm çap boyutuna sahiptirler. Mikrokürelerin karakterizasyonu TEM, X-ışın difraksiyon analiz yöntemleri ile karakterize edilmişlerdir.

Örnekler, *Escherichia coli*, *Staphylococcus aureus*, *Enterococcus faecalis*, *Bacillus cereus*, and *Pseudomonas aeruginosa* mikroplarına karşı önemli derecede antimikrobiyal aktivite gösterdiler ve *Candida albicans* mikrobına karşı herhangi bir antimikropsal aktivite gözlenemedi. Silk fibroin kullanmanın faydası ise, etkili bir protein olan fibroinin birçok biyomedikal uygulamalarında kullanılmasıdır. İpek fibroin proteininden elde edilen mikroküreler, yara iyileştirme işlevinde kurutmayı destekleyici ve steril bir ortam oluşturmalarından dolayı pek çok biyomedikal uygulamalar için uygundur.

ANAHTAR KELİMELER: İpek Fibroin, Mikroküreler, Triflorofosfat (TPP), İyonotropik Jelasyon, Antimikrobiyal Aktivite

TABLE OF CONTENTS

ACKNOWLEDGEMENT	ii
ABSTRACT	vi
ÖZET	v
TABLE OF CONTENTS	vi
LIST OF TABLES	viii
LIST OF FIGURES	ix
LIST OF ABBREVIATIONS	xi

CHAPTER 1: INTRODUCTION

1.1 General Introduction	1
1.2 A Brief Classification of Silkworms	3
1.3 Silk Processing by Silkworm	4
1.4 Properties of Silk	6
1.4.1 Mechanical properties	7
1.4.2 Biocompatibility	7
1.4.3 Biodegradability	7
1.5 Micro-sized Particles	8
1.6 Objectives of Study	9
1.7 Aim of Study	9

CHAPTER 2: MATERIALS AND METHODS

2.1 Materials	10
2.2 Preparation of Pure Silk Fibroin	10
2.2.1 Degumming Process	11
2.2.2 Dissolution Process	11
2.2.3 Dialysis Process	12
2.3 Preparation of Silk Fibroin Microparticles	13
2.4 Antimicrobial Susceptibility Testing	17
2.4.1 Disc Diffusion Method	17

2.5 Characterization of SF Microparticles	18
2.5.1 Scanning Electron Microscopy Analysis	18
2.5.2 X-ray Diffraction Analysis	18

CHAPTER 3: RESULTS AND DISCUSSION

3.1 Synthesis of Microparticles	20
3.2 SF Microparticle Characterization	20
3.2.1 Antimicrobial Susceptibility Test Results	20
3.2.2 Scanning Electron Microscopy (SEM) analysis	28
3.2.3 X-Ray Diffraction (XRD) Analysis	36
3.3 Applications	37

CHAPTER 4: CONCLUSION AND RECOMMENDATIONS

4.1 Conclusion	38
4.2 Recommendations	38

REFERENCES	39
-------------------------	----

LIST OF TABLES

Table 1.1: Different contrast in properties between the two proteins of silk from <i>B.mori</i>	7
Table 2.1: Samples with the different composite and cross-linker	15
Table 3.1: Showing the results of the antimicrobial susceptibility test supporting the above images or figure.....	27
Table 3.2: Showing the Excel sheet results of the analyzed figure 3.5.7 using the ImageJ software and further processed in OriginLab software.....	34
Table 3.3: Showing the tabulated result of the Gaussian gotten from Software called OriginLab.....	35

LIST OF FIGURES

Figure 1.1: Types of Silk, Families and species of silkworms.....	4
Figure 1.2: In vivo processing in silk glands.....	5
Figure 1.3: A simplified cycle of silkworm.....	6
Figure 2.1: The last two processes in the preparation of a pure silk fibroin solution	12
Figure 2.2: A schematic flow of the purification process to the point of microparticle formation.....	13
Figure 2.3: The basic steps involved in the process of ionic gelation.....	13
Figure 2.4: Ionotropic gelation technique setup.....	16
Figure 2.5: A native fiber showing aligned beta-sheet crystallites and an amorphous region.....	19
Figure 3.1.1: Shows the zone of inhibition for sample C _{0.05}	21
Figure 3.1.2: Shows the zone of inhibition for sample C _{0.10}	22
Figure 3.1.3: Shows the zone of inhibition for sample C _{0.15}	22
Figure 3.1.4: Shows the zone of inhibition for sample C _{0.20}	23
Figure 3.2.1: Shows the zone of inhibition for sample F _{0.05}	23
Figure 3..2.2: Shows the zone of inhibition for sample F _{0.10}	24
Figure 3..2.3: Shows the zone of inhibition for sample F _{0.15}	24
Figure 3.2.4: Shows the zone of inhibition for sample F _{0.20}	25
Figure 3.3.1: Shows the zone of inhibition for sample negative control which is SF MPs without drug.....	25
Figure 3.3.2: Shows the zone of inhibition of one of the positive control which is drug Cipro.....	26
Figure 3.3.3: Shows the zone of inhibition of the other positive control which is drug Floxin.....	26
Figure 3.4: A bar graph presentation of the antimicrobial activity.....	28
Figure 3.5.1: Shows SEM micrograph of sample C _{0.20} of 1µm at x10 magnification....	29

Figure 3.5.2: Shows SEM micrograph of sample C _{0.20} of 5µm at x5 magnification.....	30
Figure 3.5.3: Shows SEM micrograph of sample C _{0.20} of 10µm at x2.5 magnification..	30
Figure 3.5.4: Shows SEM micrograph of sample C _{0.20} of 10µm at x1 magnification....	31
Figure 3.5.5: Shows SEM micrograph of sample C _{0.20} of 100µm at x100 magnification.....	32
Figure 3.5.6: Showing SEM micrograph of sample C _{0.20} of 1µm at x20 magnification...	32
Figure 3.5.7: SEM micrograph duplicated from figure 3.5.5 and filtered for better analysis when using software ImageJ to calculate particle diameter.....	33
Figure 3.5.8: Gaussian plot showing the various diameters from the resized image in figure 3.5.7.....	35
Figure 3.6: The XRD analysis result of the SF MPs.....	37

LIST OF ABBREVIATIONS

ABCs:	Amphiphilic Block Copolymers
Ala:	Alanine
ATCC:	American type culture collection
<i>B. cereus:</i>	<i>Bacillus cereus</i>
<i>B .mori:</i>	<i>Bombyxmori</i>
<i>C. albicans:</i>	<i>Candida albicans</i>
CIP:	Ciprofloxacin (Cipro)
cm:	Centimetres
<i>E.coli:</i>	<i>Escherichia coli</i>
<i>E. faecalis:</i>	<i>Enterococcus faecalis</i>
Gly:	Glycine
IG:	Ionic gelation or ionotropic gelation
MPs:	Microparticles
OFX:	Ofloxacin (Floxin)
<i>P. aeruginosa:</i>	<i>Pseudomonas aeruginosa</i>
<i>S. aureus:</i>	<i>Staphylococcus aureus</i>
SEM:	Scanning Electronic Microscopy
Ser:	Serine
SF:	Silk fibroin
TPP:	Sodium Triphosphate Pentabasic
XRD:	X-ray diffraction

CHAPTER 1

INTRODUCTION

1.1 General Introduction

A biomaterial is a substance which is engineered into a form, alone or as part of a complex system, to interact with a desired biological system. These biomaterials are often fabricated or designed into medical devices to help in tissue regeneration, to augment the function of a tissue and, in some cases, to even replace the tissue. They are also used in the development of biomolecule delivery. Cells attach and migrate along the biomaterial platform. These biomaterials can be broadly classified into natural and synthetic biomaterials (Talukdar and Kundu, 2014). Biomaterials are obtained from a wide range of sources. Chitosan, collagen, keratin, elastin, and silk are some of the major natural polymers studied for use as biomaterial (Sionkowska, 2011). For years silk has been used in different ventures, biomedically the use of silk has advanced greatly as biomaterials are used in tissue engineering for scaffold preparation, contact lenses, wound dressings, and controlled release of drugs. Silkworms, spiders, scorpions, mites, and flies, each produces a distinct variety of silk by several different larvae in the order *Lepidoptera* (Altman et al., 2003). Prasad et al. (2005) mentioned that most of the world's silk used for textile and other applications is produced by the domesticated *Bombyx mori* silkworm.

Silk are a natural polypeptide composite material consisting of two major proteins, fibroin, and sericin. The raw silk has a structure of two parallel fibroin fibers linked by disulfide bonds and held together with successive sticky layers of sericin on their surfaces that help in the formation of a cocoon. Fibroin has been used in textile manufacturing and for several biomaterial applications, whereas sericin is considered a waste material in the textile industry.

Sericin or silk glue is a globular protein that makes up 25 to 30% of silk proteins, consisting of 18 amino acids having strong polar side chains (hydroxyl, carboxyl, and amino groups). Its highly hydrophilic nature is as a result of the high content of serine

(~33.4%) and aspartic acid (~16.7%) in sericin (Aramwit et al., 2012). Sericin had initially been disregarded as a biomaterial because of several proposed allergenic activity. Researchers have banished this misconception, proving the biocompatibility of sericin and presently it is still irrefutable (Chirila et al., 2013).

Fibroin, which is the central core is coated with a covering of sericin. Silk protein has similarities with proteins like collagen, elastin, keratin, fibroin and sporgin and is an essential constituent of cocoon filament. The demand for biocompatible, biodegradable and bioresorbable materials has increasingly appreciated over the last decade. A suitable biomaterial has to be non-immunogenic, biocompatible and biodegradable, and also can be functionalized with bioactive proteins and chemicals. Specifically, biodegradability is an important property of this biomaterial. Natural biodegradable polymers like collagen, gelatin, chitosan and silk fibroin have promising advantages over synthetic polymers due to their distinguishing properties, including excellent biocompatibility, biodegradability, and bioresorbability. Their physical and chemical properties can be easily modified to achieve desirable mechanical and degradation characteristics (Thirupathamma et al., 2013).

Silk fibroin purified from the cocoons of *Bombyx mori* silkworm has been used as suture material for decades. The fibrous protein, silk fibroin is composed of glycine and alanine as the main amino acid residues. Moreover, it has been extensively investigated because of its favorable mechanical and structure properties, biological compatibility and biodegradability (Meinel et al., 2005).

The silk fibroin is a natural polymer that has been used for its high tensile strength, biocompatibility, and other physicochemical properties. It has high capability to form structures such as biofilm, scaffold, grafts, nanoparticle, microparticle, and nanofiber. The silk fibers were coated with sericin that is a gum-like protein. Sericin protein works as the glue that is intended to maintain the cocoon's structure (Pérez-Rigueiro et al., 2001).

These various forms have been affirmed to promote cell migration, adhesion, proliferation, and promote tissue repair *in vivo*. The biofilm form of the silk fibroin is an essential form of it. Its usage has expanded the use of silk-based biomaterials as promising biofilms for tissue engineering applications ranging from artificial skin, ligament,

connective tissues like skin cell culturing, and also in drug delivery system. The silk fibroin Biofilms can exhibit perfect environmental adaptation for cell growth because of the porous structure of the silk fibroin biofilms. This enables integration of cells within the biomaterial. So, the silk fibroin biofilms are useful in a broad range of medical applications (Liu et al., 2007).

1.2 A Brief Classification of Silkworms

The ranking of silkworms into mulberry and non-mulberry silkworms comes from the feeding habit of the silk-producing insects from the members of the families Saturniidae and Lasiocampidae, which are non-mulberry silkworms. Mulberry silkworms belong to the family Bombycidae, and the silk is called mulberry silk. Commercially available mulberry silk was produced from one single species called *Bombyx mori*. Mulberry silkworms were entirely domesticated, and they do not occur naturally. They need human care for their growth and reproduction (Mahendran et al., 2006). The larvae prefer to eat white mulberry (*Morus alba*) though they can also eat the leaves of other *Morus* species. Silkworms require a complete diet, containing four main constituents. The feeding leaves must contain fiber, saccharides, water and resin. The first three nourishes the worm and fourth component help in preparing silk.

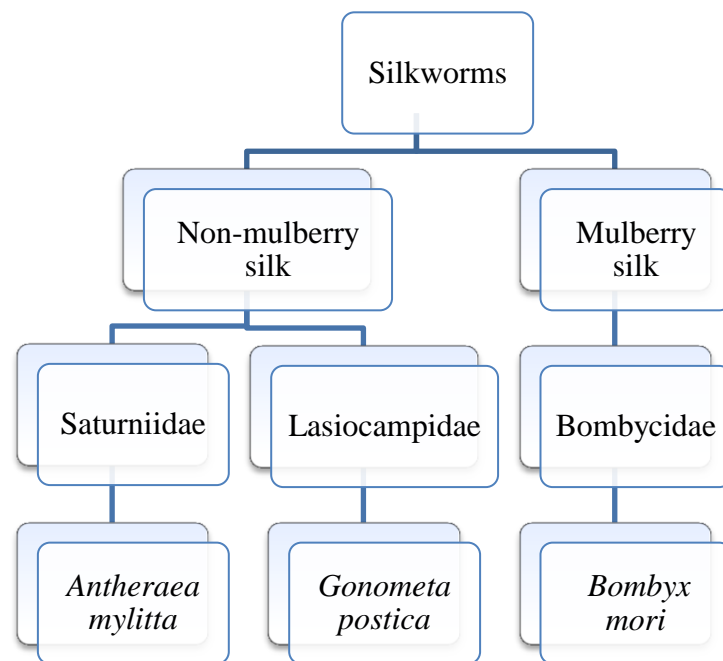


Figure 1.1: Types of Silk, Families and species of silkworms

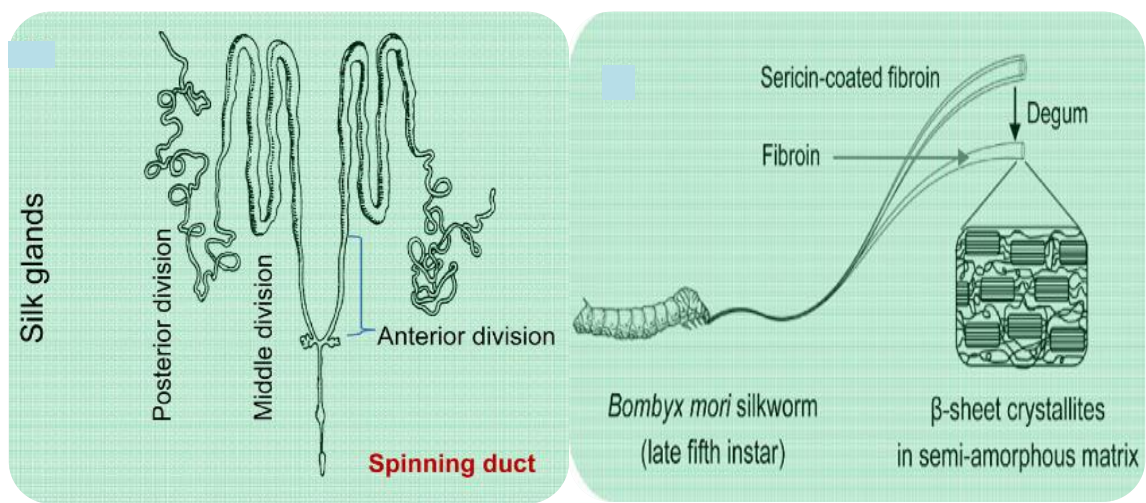
1.3 Silk Processing by Silkworm

The silk spinning organ of the silkworm consists of two large glands, situated laterally along its sides, under the alimentary canal. The glands made of glandular epithelium and are surrounded by two layers of cells. Each gland has three parts (see Fig. 1.2a):

- Posterior (15 cm in length, consists of 500 secretory cells, secretes protein fibroin);
- Middle (7 cm in length, consists of 300 secretory cells, secretes protein sericin);
- Anterior (2 cm in length, consists of 250 secretory cells, secretes protein sericin).

A cocoon formed in 2–5 days of the complete spinning process can vary depending on the season. Initially, a loose shell form is wound by the silkworm around itself. The silkworms then start more consistent and compact spinning after covering the body inside the cocooning's shell. After three days of complete spinning, the worms transform themselves into chrysalis form by shedding the skin for the last time and entering a hibernating stage.

The pupa remains inside the cocoon depending upon the voltinism of the variety. Between 15 and 20 days later, the pupa wakes up and emerges from the cocoon in the form of a moth, with an entirely different physiology and morphology (Winsted Silk Co., 1915). The size of *B. mori* cocoons is about 30–35 mm. Cocoons of *B. mori* can be found in different colors, such as white, bright yellow, pale yellow, creamy white and of greenish hue (Winsted Silk Co., 1915).



(a) In vivo processing in silk glands (b) Natural spinning by silkworms
Figure 1.2: Production of fibroin fibers with unique features (Koh et al., 2015)

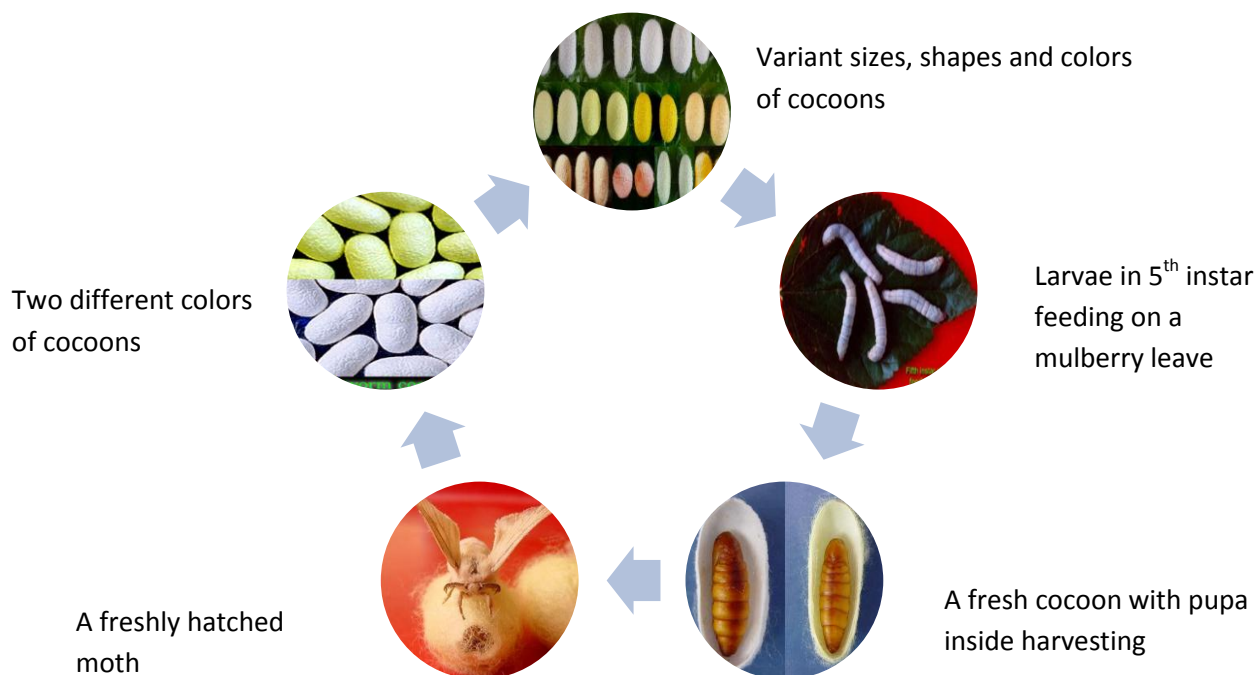


Figure 1.3: A simplified cycle of silkworm showing different shapes and shades of cocoons (Prasad et al., 2005)

1.4 Properties of Silk

Silkworm *B. mori* is one of the best-characterized silk is the cocoon silk from the domesticated. The silk from the cocoons of *B. mori* is made of two structural proteins, the heavy chain (~325 kDa) and light chain (~25 kDa). The chains are held together by the glue-like proteins known as sericin (20 kDa to 310 kDa). The heavy chain of silk fibroin contains alternating hydrophobic and hydrophilic blocks similar to those seen in amphiphilic block copolymers, ABCs (Wenk et al., 2010).

Table 1.1: Different contrast in properties between the two proteins of silk from *B.mori*

Protein	Sericin	Fibroin
Type of protein	Glue-like protein	Structural protein
Percentage proportion in cocoon	20-30%	70%
Structural properties	Hydrophilic; stays in its partially unfolded state, consisting of random coil structure in high proportion (Okazaki et al., 2011)	Hydrophobic; β -sheet and α -helices (Lawrence, 2014)
Composition	Polypeptide polymer containing 18 amino acids (Okazaki et al., 2011).	Amino acids in a heavy chain and a light chain in a ratio 1:1 linked with disulfide bonds (Hu and Kaplan, 2011)
Molecular weight	24-250kDa	26-370kDa
Major properties	Antibacterial, UV-absorbing, high moisture absorbancy, antioxidant, antitumor, wound-healing (Hazeri et al., 2012).	Biocompatible, biodegradable, crystallinity, mechanical properties and opportunity for chemical functionalization (Pritchard and Kaplan, 2011).

1.4.1 Mechanical properties

Lawrence (2014) reported that the unique feature of fibrous proteins is the β -sheet crystallinity that enables the fibers to retain its flexibility alongside their remarkable strength. From the perspective of an evolutionary structural function, the organization of β -sheet crystals within the fibers provides the strength and durability to support and protect the transforming worm inside the *B. mori* cocoon. It is these robust mechanical properties

that make silk particularly attractive for use in tissue engineering applications where mechanical integrity is a primary concern.

1.4.2 Biocompatibility

Biocompatibility is the ability of a biomaterial to achieve a suitable host response in a particular application (Williams, 1999). Biocompatibility assesses the degree and time frame of the adverse changes in homeostatic mechanisms that govern the host response. In simple terms, it predicts whether a biomaterial poses a potential harm to the host (Aramwit, 2014). The host response covers a broad range of responses that the body will have to implant foreign material. General indicators of a biocompatible material are low and non-sustained inflammatory response, low cell toxicity, and low thrombosis formation (Bailey, 2013).

1.4.3 Biodegradability

Biodegradability is employed to ascertain the degree of degeneration of silk materials. Vert et al. (1992) defined biodegradability as the degradability of an implanted polymer by the fragmentation of biological elements, which is carried away from its site of the implant via movement of fluid but not essentially out of the body. Furthermore, the complete eradication of preliminary foreign materials via metabolization or filtration of the degraded bio-products is called bio-sorption (Vert et al., 1992). Several research works have shown the *in vivo* degradability of silk (Wang et al., 2008).

1.5 Micro-sized Particles

Zhang and Guan (2011) reported Size plays a major role in the transportation of particles, uptake at cellular levels, and degradation. Particle size affects degradation by influencing penetration of water and clearance rate of degradation products, which can catalyze degradation reaction. The particle size plays an important role in its effectiveness (Li et al., 2011). Rajkhowa and Wang (2014) also reported that particle size depended on the production method. The particle sizes in this work are between 1 and 1000 micrometers or microns. The micro size of the particles will aid interaction with other molecules or compounds at molecular and cellular levels

1.6 Objective of the Study

In this research work, pure silk fibroin synthesized from cocoons of *B.mori* silkworm is loaded with two antimicrobial drugs in different ratios using crosslinking agent TPP to form microparticles in a process called ionic gelation. These microparticles are then used to carry out antimicrobial susceptibility test to measure and compare the various zone of inhibition. The wide spectrum of microorganisms used are namely *Escherichia coli* (ATCC 25922), *Candida albicans* (ATCC 90028), *Staphylococcus aureus* (ATCC 25923), *Enterococcus faecalis* (ATCC 29212), *Bacillus cereus* (ATCC 10876), and *Pseudomonas aeruginosa* (ATCC 27853).

1.7 Aim of the Study

This research is aimed at the following;

- 1) Determining the morphology and particles size of formed microparticles.
- 2) Determining the ability of SF alone and SF loaded microparticles susceptibility to a wide spectrum of microbes.
- 3) comparing inhibition activities between SF MPs, SF loaded with Cipro and Floxin, Cipro and Floxin alone.
- 4) Determining which microorganism is more sensitive to the different spectrum of microparticles.
- 5) Providing a point of reference for other researchers on the subject in the future.

CHAPTER 2

MATERIALS AND METHODS

2.1 Materials

The cocoons were purchased from Büyük-Han (translated “Great Inn”) located at one of the major trade area in the city of Lefkoşa, Turkish Republic of North Cyprus (TRNC). The chemicals used in this study are of high purity and standard based on the track record of the companies they were purchased from namely Merck and Sigma. Anhydrous sodium carbonate and calcium chloride anhydrous powder from EMSURE® Merck chemicals in Darmstadt, Germany were used for this analysis. Also including sodium triphosphate pentabasic and Mueller-Hinton agar purchased from SIGMA-ALDRICH. Floxin® (Ofloxacin) and Cipro® (Ciprofloxacin) were purchased from a reliable pharmaceutical outlet. Deionized water was used during the whole experimental process. Also, all the glass wares used were properly washed and afterward left to dry in a hot air oven.

2.2 Preparation of Pure Silk Fibroin

The processes involved in the synthesis of the pure silk fibroin are as follows:

- Degumming process
- Dissolution process
- Dialysis process

This three D’s are the processes involved to obtain the pure silk fibroin for the formation of our microparticles.

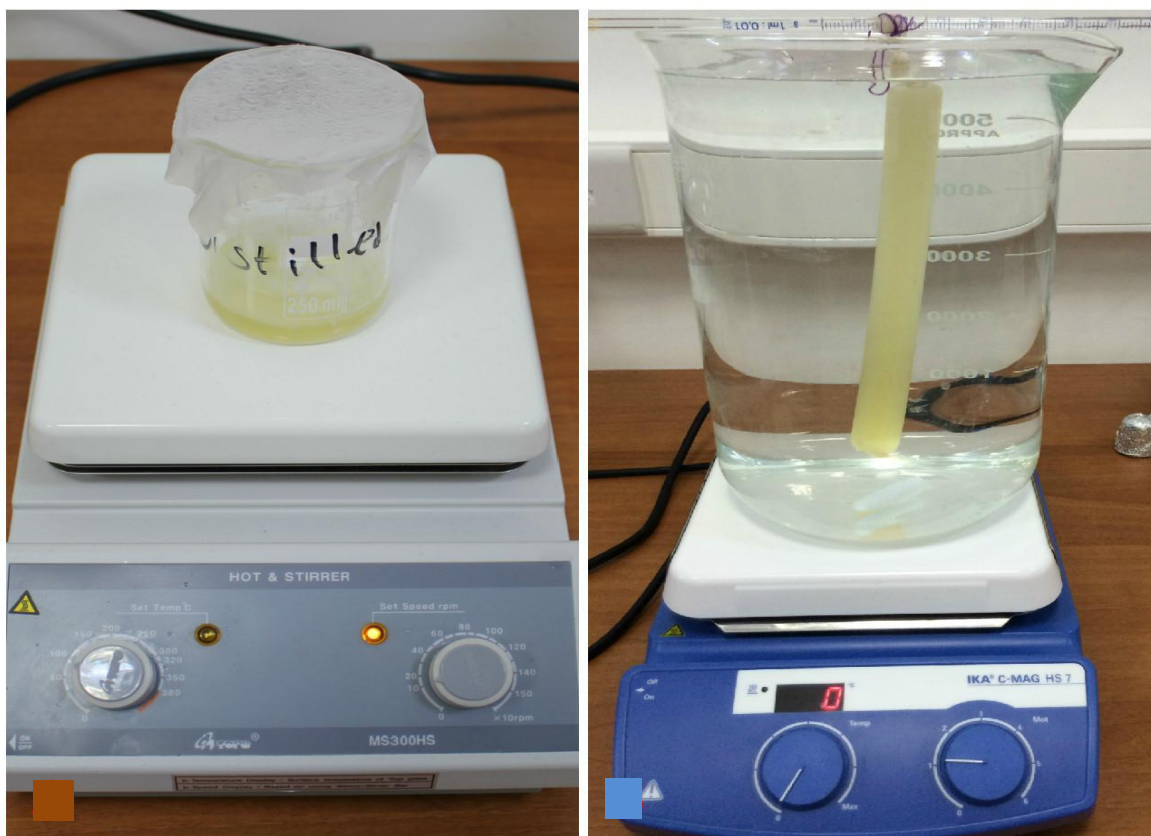
2.2.1 Degumming Process

Wenk et al. (2010) reported that the degumming process involves boiling silk in an alkaline solution that gradually separates sericin from the silk due the high hydrophilic nature of sericin. The degumming process does not affect the secondary structure of silk fibroin (Ayutsede et al., 2005).

As stated earlier, the main aim of the degumming process is to remove the gum, sericin hence the name degumming. 5.3 grams dissolved in 500 ml of deionized water to yield 0.1 M of sodium carbonate solution is prepared and used in this process (Jasmine and Mandal, 2014). The cocoons were first cut into smaller pieces, and 1 g of the cocoon is weighed and put into a conical flask. Then 100 ml of the 0.1 M sodium carbonate Na_2CO_3 solution (1 g / 100 ml w/v) were added into the same conical flask. A magnetic stirring bar was added to the mixture and place on the magnetic stirrer that is set to 70 $^{\circ}\text{C}$ at 1rpm for three hours; this is the first of three rounds to complete the process of degumming. The process is repeated to ensure that sericin; the gum is entirely removed from the silk cocoon leaving us with silk fibroin that is left to dry at room temperature.

2.2.2 Dissolution Process

The dissolution process changes the state physical state of the silk fibroin from solid to liquid and also the chemical state by breaking the long polypeptide chains of the silk fibroin into shorter ones. The process involves the use of an electrolyte solution consisting of 29.15 ml of ethanol $\text{C}_2\text{H}_5\text{OH}$, 27.75 g of calcium chloride CaCl_2 and 36 ml of deionized water H_2O . After the electrolyte solution is prepared, the volume of electrolyte solution needed to get 6 % silk solution (6 g / 100 ml w/v) is measured. The required grams of silk fibroin to make up 6 % was calculated and gradually added to the electrolyte solution of proportional volume while on the magnetic stirrer at 75 $^{\circ}\text{C}$ and 1 rpm. This continues till the silk fibroin is totally dissolved, hence the end of the dissolution process.



(a) The dissolution of Silk fibroin

(b) a dialysis process setup

Figure 2.1: The last two processes in the preparation of a pure silk fibroin solution

2.2.3 Dialysis Process

The dialysis process completes the whole process of pure silk fibroin synthesis by removal of ions which resulted from earlier reactions. A carboxymethyl cellulose semipermeable membrane tube used to enable the removal or escape of ions from the silk fibroin solution, hence giving us our pure silk fibroin solution. The impure silk fibroin is measured and put into the tube using a funnel and tied properly to avoid leakage. It was then put into a 5 litre glass beaker containing deionized water with a magnetic stirring bar inside it already. Then placed on a magnetic stirrer at 0 °C (but acted upon by a room temperature of about 37°C) and 1 rpm for 3 hours then the deionised water is changed for another round and then the last round to total three rounds. The pure silk fibroin is removed from the membrane using a syringe; it is then ready for use.

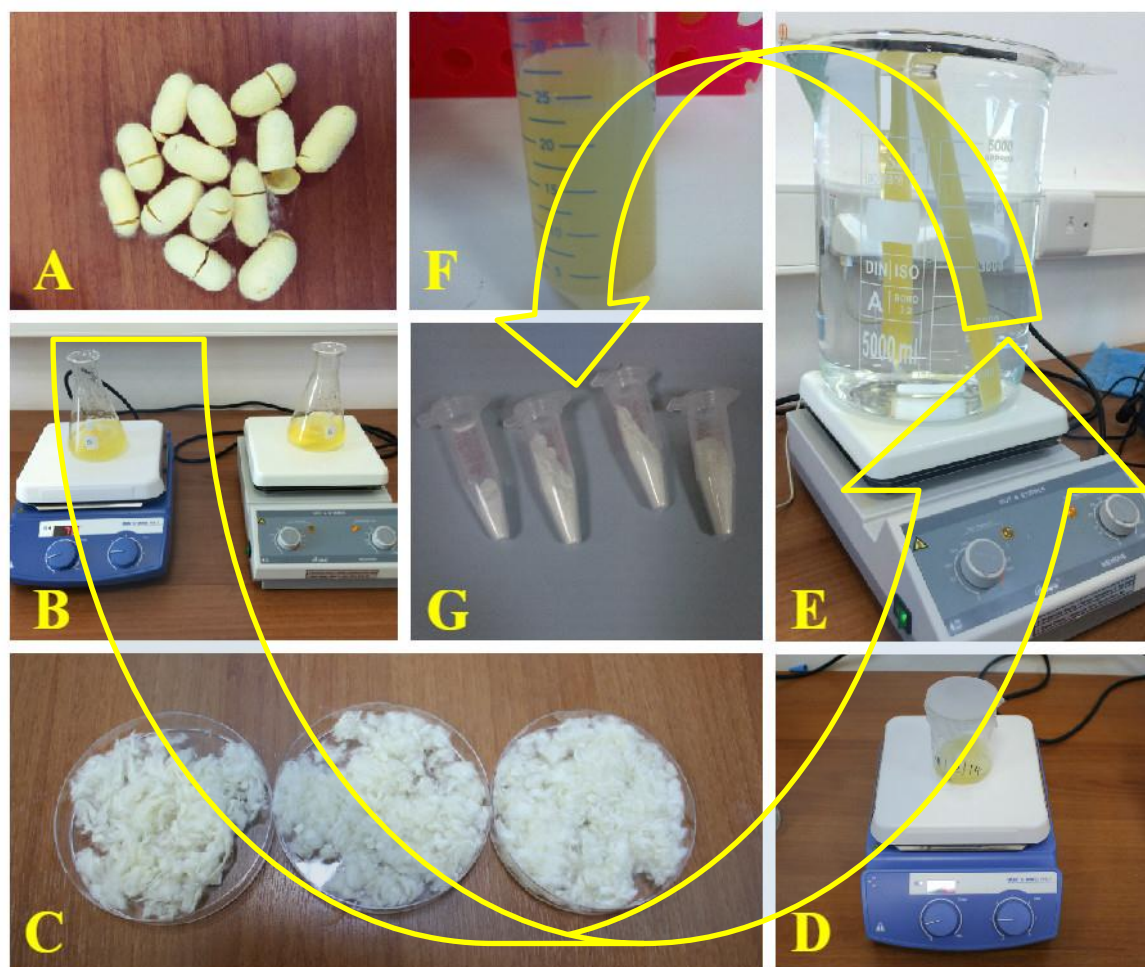


Figure 2.2: A schematic flow of the purification process to the point of microparticle formation

2.3 Preparation of Silk Fibroin Microparticles

The microparticles are prepared by a method of Ionic gelation or Ionotropic gelation which is the formation of microparticles based on the ability of polyelectrolytes to cross link in the presence of counter ions which in this case is 0.1M of sodium triphosphate pentabasic $\text{Na}_5\text{P}_3\text{O}_{10}$ (Patil et al., 2012). It was prepared by weighing 7.36 g and dissolving it into 200 ml of deionized water to yield the 0.1M solution of it.

According to Kunjachan and Jose (2010), IG is a method frequently used for synthesis of chitosan microparticles and nanoparticles and also was used in Incorporating chitosan and

TPP into SF as seen in the publication by Chung et al. (2011). Hence the motivation to use this technique in a slightly different way from how it has been used before based on the literature survey been done. The drugs used in this project are Floxin and Cipro, which are both tablets of an antibiotic drug in the same family of fluoroquinolones. The active ingredient in Floxin is Ofloxacin and in Cipro is Ciprofloxacin. These two drugs were used for their availability and potency. As shown in the table and figure below, the volume of SF is constant as well as the volume of the crosslinking solution of TPP. The major difference is the weight of the drug used in grams.

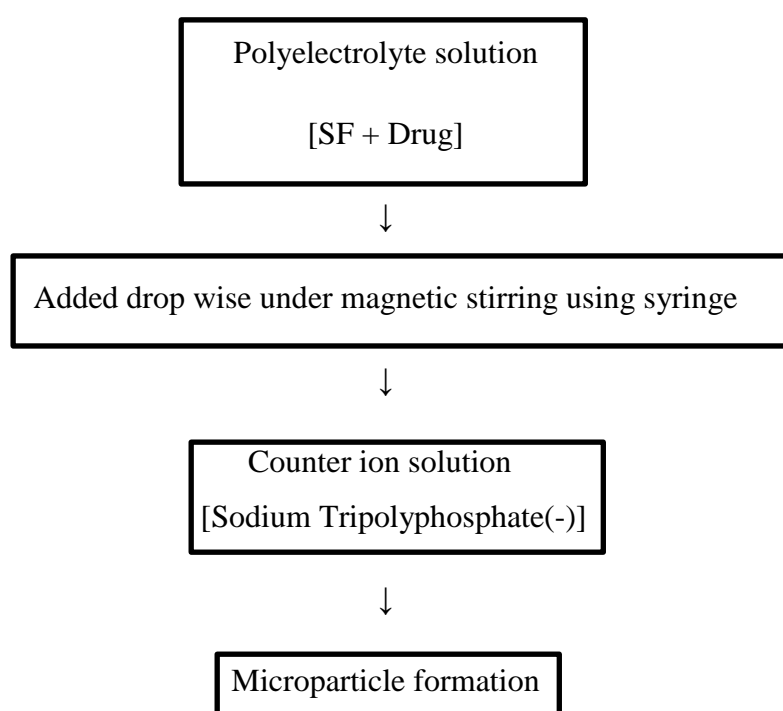


Figure 2.3: The basic steps involved in the process of ionic gelation (Patil et al., 2012)

Table 2.1: Samples with the different composite and cross-linker

Samples	Silk Fibroin (ml)	Cipro (grams)	Floxin (grams)	0.1 M of TPP solution (ml)
C_{0.05}	2.0	0.05	-	50
C_{0.10}	2.0	0.10	-	50
C_{0.15}	2.0	0.15	-	50
C_{0.20}	2.0	0.20	-	50
F_{0.05}	2.0	-	0.05	50
F_{0.10}	2.0	-	0.10	50
F_{0.15}	2.0	-	0.15	50
F_{0.20}	2.0	-	0.20	50
Control	2.0	-	-	50

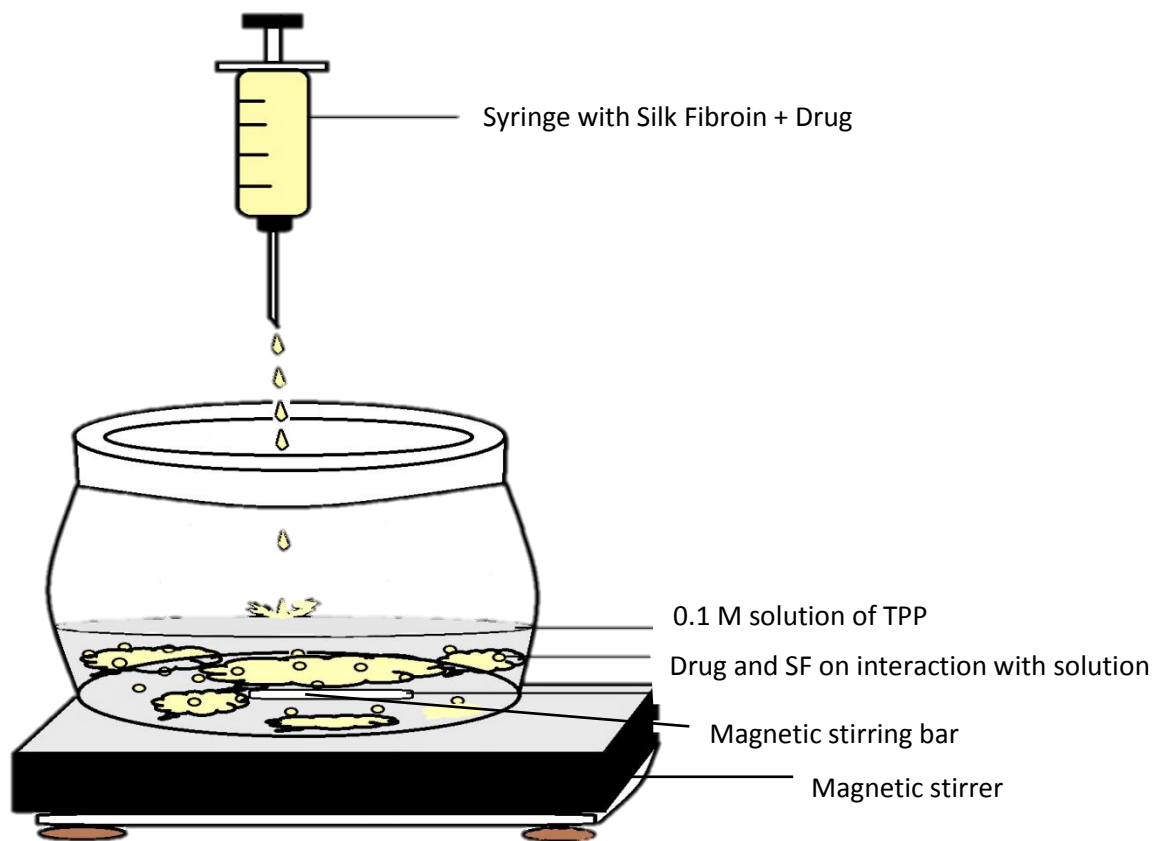


Figure 2.4: Ionotropic gelation technique setup

Four different ratios of the drugs (0.05 g, 0.10 g, 0.15 g, and 0.20 g) were mixed independently with 2 ml of the pure silk fibroin for the process to kick-start. After that 50 ml of already prepared 0.1 M of sodium triphosphate pentabasic $\text{Na}_5\text{P}_3\text{O}_{10}$ solution was separated for use from the bulk of the solution. 50 ml was the volume of the crosslinker used for each portion of the mixture of drug and silk fibroin throughout the process. A 2.5 ml syringe is using to incorporate the mixture of drug and silk fibroin into the crosslinker solution in drops. With every drop, a visible cloud is seen which later settles and after a 12 hour period the samples are filtered and the residue is scooped and dried in a petri dish at room temperature. The dried sample is later grinded and put into a labeled plastic vial.

The samples were been sterilized by a method of dry sterilization so as to ensure that samples are microbe free for the antimicrobial activity tests.

2.4 Antimicrobial Susceptibility Testing

2.4.1 Disc Diffusion Method

Antimicrobial susceptibility tests are conducted to determine the *in vitro* activity of an antimicrobial material against certain microbial species. The antimicrobial susceptibility tests in this research was carried out with six microorganisms, five of which were bacteria (3 gram positive and 2 gram negative) and one of which was a yeast or fungus. They are namely *Staphylococcus aureus* (ATCC 25923), *Enterococcus faecalis* (ATCC 29212), *Bacillus cereus* (ATCC 10876), *Pseudomonas aeruginosa* (ATCC 27853), *Escherichia coli* (ATCC 25922), and *Candida albicans* (ATCC 90028) respectively. Mueller Hinton agar was used instead of other agar such as nutrient agar, chocolate agar, blood agar, and so on based on Clinical and Laboratory Standards Institute's (CLSI) (2012) for antimicrobial susceptibility testing.

Firstly, the solid agar medium of Mueller Hinton Agar (Merck, Germany) was prepared according to the manufacturer's guideline of 34.0 g/L and then sterilized by autoclaving at 121°C for 15 minutes. Afterwards it is poured into the petri dishes at a depth of approximately 4mm and when cool enough, it is placed in the refrigerator and left overnight. A PhoenixTM ID broth of all the microorganisms to be used is prepared to a standard of 0.5 McFarland (approximately 10⁶ cells/ml) which is measured using a BD PhoenixSpec Nephelometer. The agar plate is then labelled and using a sterile cotton swab on its surface to inoculate it with 10 µL of ID broth containing a specific microorganism.

For easy incubation of the samples on the sterilised paper discs, 0.1 grams of each sample was diluted with 1ml of ultrapure water. Using a sterile tip on the micropipettor for each sample to avoid error in the results, 20 µL of diluted samples were measured using the micropipettor and poured onto the blank disc that has been placed on the inoculated agar.

When all of the samples are carefully placed in the culture media inoculated with the different microorganisms. They are placed at room temperature for 10 minutes and then incubated upside down at 37±0.1°C for 24 hours. After 24 hours results were readily visible. Note that the negative control is SF MP only without drug and the positive controls are Floxin and Cipro separately.

2.5 Characterization of SF Microparticles

2.5.1 Scanning Electron Microscopy Analysis

Scanning electron microscopy (SEM) is employed in order to observe surface topography and morphology of the MPs. The electrons in this analysis scan from the top in a beam fashion, focusing on the sample from one point to another and resulting in refracted electrons.

The Scanning Electron Microscopy analysis was done at TÜBİTAK- Marmara Research Centre at Gebze, Istanbul, Turkey by using a SEM Model Jsm- 6510 model at an acceleration voltage 10kV.

2.5.2 X-ray Diffraction Analysis

A variety of techniques are available to study the secondary structure of silk in forms ranging from model peptides to native spun fibers. The crystalline properties of the beta-sheets are mainly studied by X-ray diffraction (XRD). Among the first to observe that fibers of silk fibroin can diffract X-rays were Herzog and Jancke (1920). Early X-ray diffraction studies of native fibers revealed the presence of an orthorhombic unit cell ($a = 9.40 \text{ \AA}$ in the hydrogen bond direction, $b = 9.20 \text{ \AA}$ in the sheet stacking direction intersheet distance and $c = 6.97 \text{ \AA}$ in the chain and fiber axis direction) (Brill, 1943; Marsh et al ., 1955) which was suggested to arise from anti-parallel beta-sheet stacking within the crystalline domains as shown in Figure below.

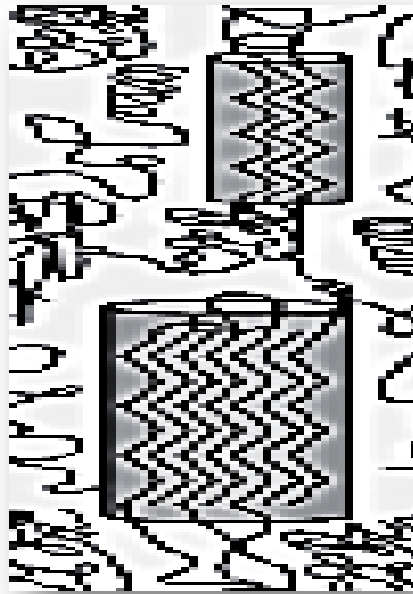


Figure 2.4: A native fiber showing aligned beta-sheet crystallites and amorphous region

X-ray diffraction was done at TÜBİTAK-MAM Gebze, by using a shimadzu XRD-600 model diffractometer with a Cu- X-ray tube ($\lambda=1.5405\text{\AA}$).

CHAPTER 3

RESULTS AND DISCUSSIONS

3.1 Synthesis of Microparticles

The IG method that resulted in the preparation of silk fibroin based microparticles containing antibiotics CIP and OFX. The following four steps lead to the synthesis of the microparticles:

- (1) Polyelectrolyte solution formed by the mixture of drug and pure silk fibroin;
- (2) Adding the solution resulting from step one using a 2.5 ml syringe into a crosslinking solution (0.1M TPP solution) in drops under the magnetic stirrer
- (3) Formation of Counter-ionic solution, and
- (4) polymerization of the microparticles.

3.2 SF Microparticle Characterization

The samples underwent characterizations by Scanning Electron Microscopy (SEM), X-ray Diffraction (XRD) Analysis and antimicrobial analysis revealing the size of the microparticles and its structure. The antimicrobial activity of the samples based on their potential to allow or inhibit the microbial growth was analyzed. Although there are different methods to test the antimicrobial activity, in this experiment the Kirby-Bauer method based on the diffusion of antibiotics through a small disc. We believe that these microparticles will be useful for wound healing and drug delivery that require microparticles with high antimicrobial property.

3.2.1 Antimicrobial Susceptibility Test Results

The results after 24 hours were good; all the samples showed a zone of inhibition except the samples incubated with the yeast. Silk fibroin microparticles (SF MPs) alone without the drug served as negative control and exhibit excellent antibacterial susceptibility. The positive control of both drugs alone also showed a larger zone of inhibition and Cipro shockingly had a 1.4 cm zone of inhibition against *Candida albicans*, the yeast that was

resistant to the all the SF MPs containing the drug. Note that silk fibroin microparticles loaded with a drug against *Enterococcus faecalis* had a zone of inhibition difficult to see and was almost regarded as not being susceptible, till when accidentally held up at an angle towards a source of light. Hence, the circular markings on the Petri dish to emphasize the zone of inhibition as seen in the figures below.

The figures below were put together in batches in regards to the of drug (0.05, 0.10, 0.15, and 0.20) contained in SF MPs, negative and positive control. In a batch, the order of the Images alphabetically points to a particular microorganism and stays the same throughout.

- A. *Escherichia coli* (ATCC 25922)
- B. *Enterococcus faecalis* (ATCC 29212)
- C. *Bacillus cereus* (ATCC 10876)
- D. *Pseudomonas aeruginosa* (ATCC 27853)
- E. *Staphylococcus aureus* (ATCC 25923)
- F. *Candida albicans* (ATCC 90028).

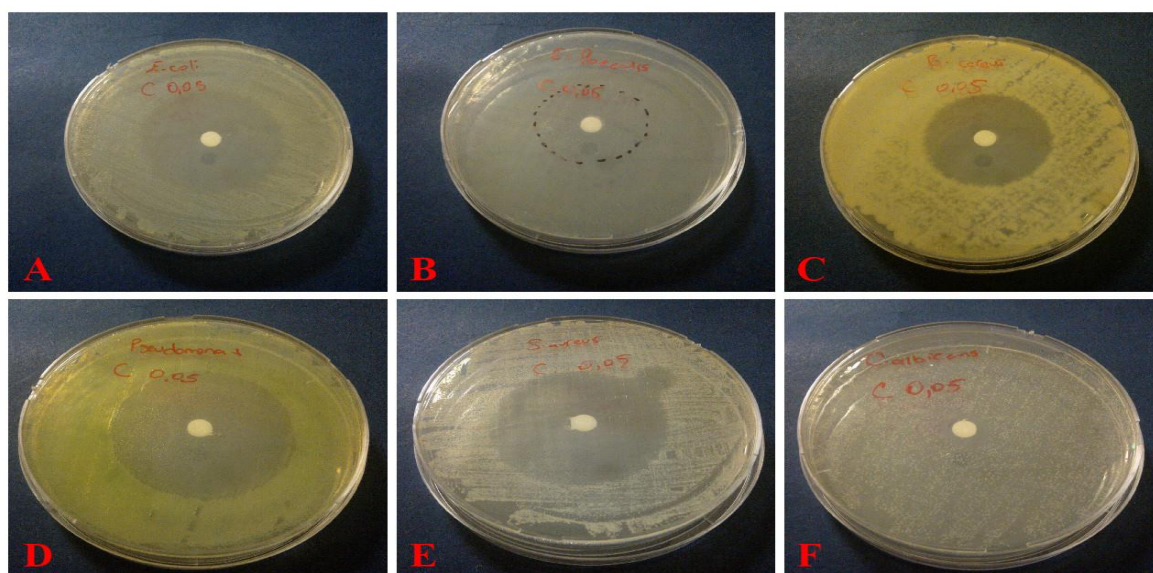


Figure 3.1.1: Shows the zone of inhibition for sample C_{0.05}

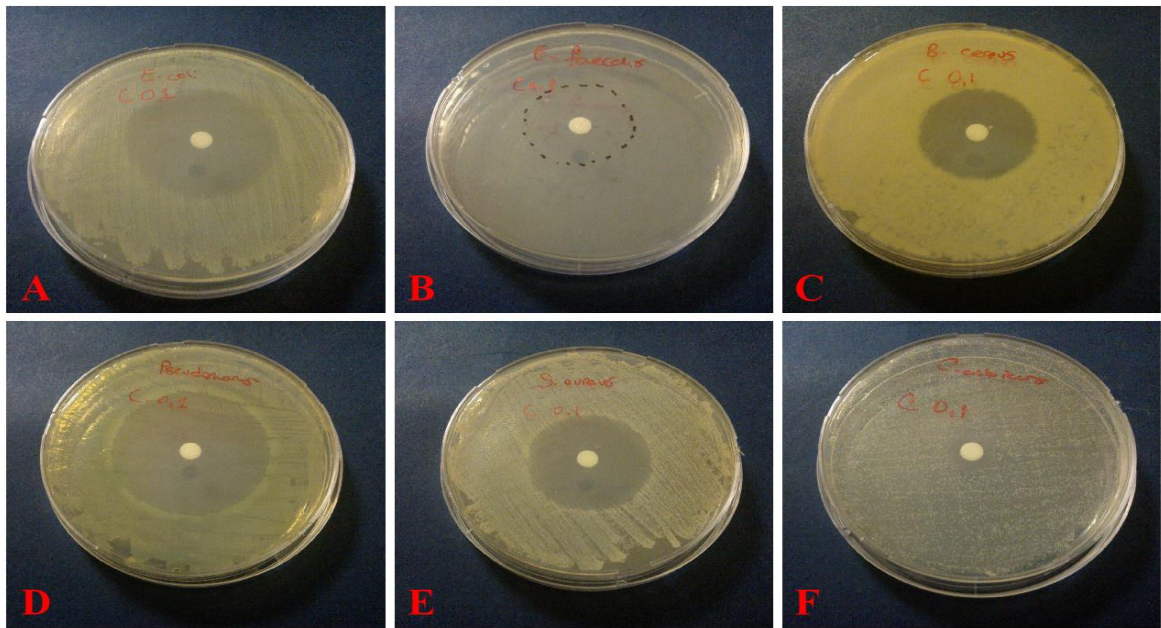


Figure 3.1.2: Shows the zone of inhibition for sample $C_{0.1}$

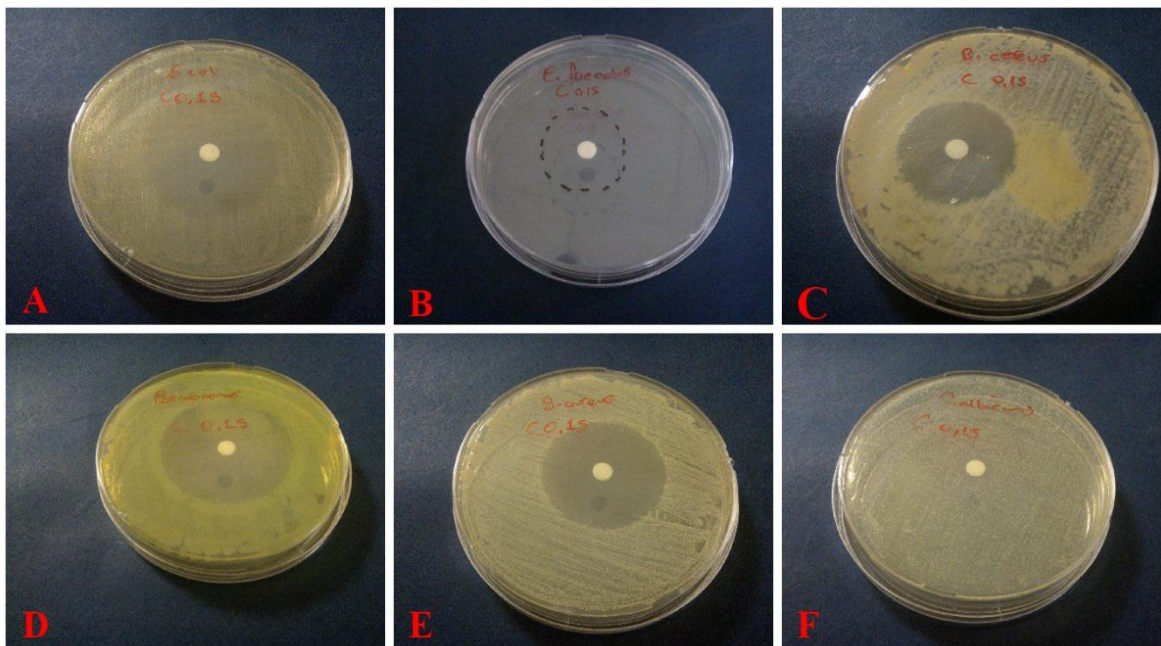


Figure 3.1.3: Shows the zone of inhibition for sample $C_{0.15}$

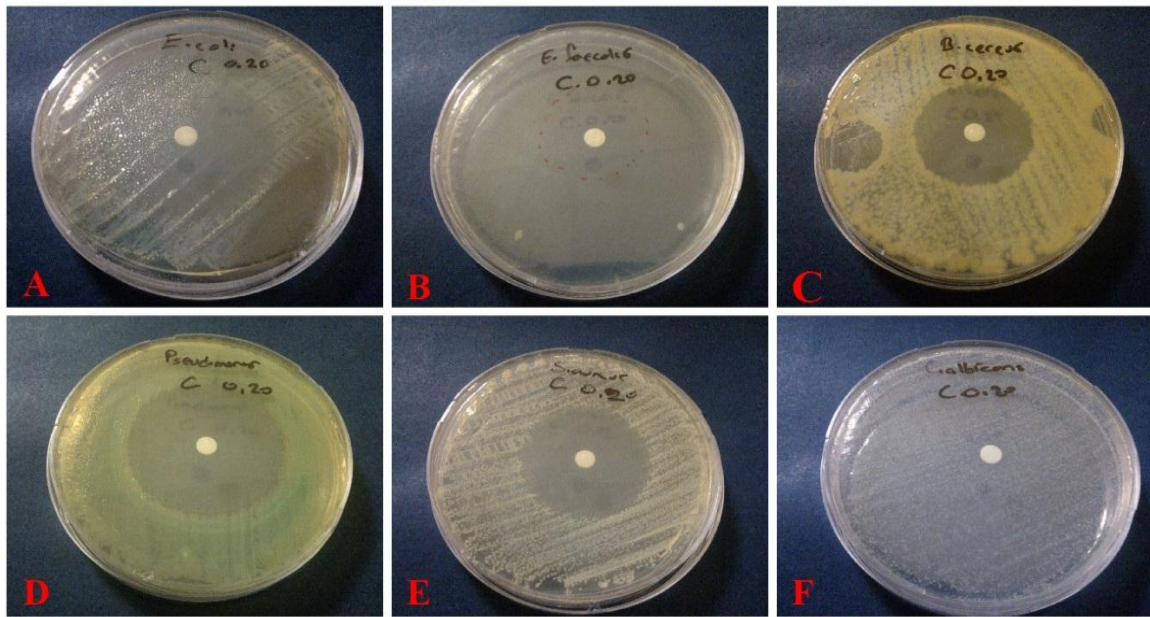


Figure 3.1.4: shows the zone of inhibition for sample $C_{0.20}$

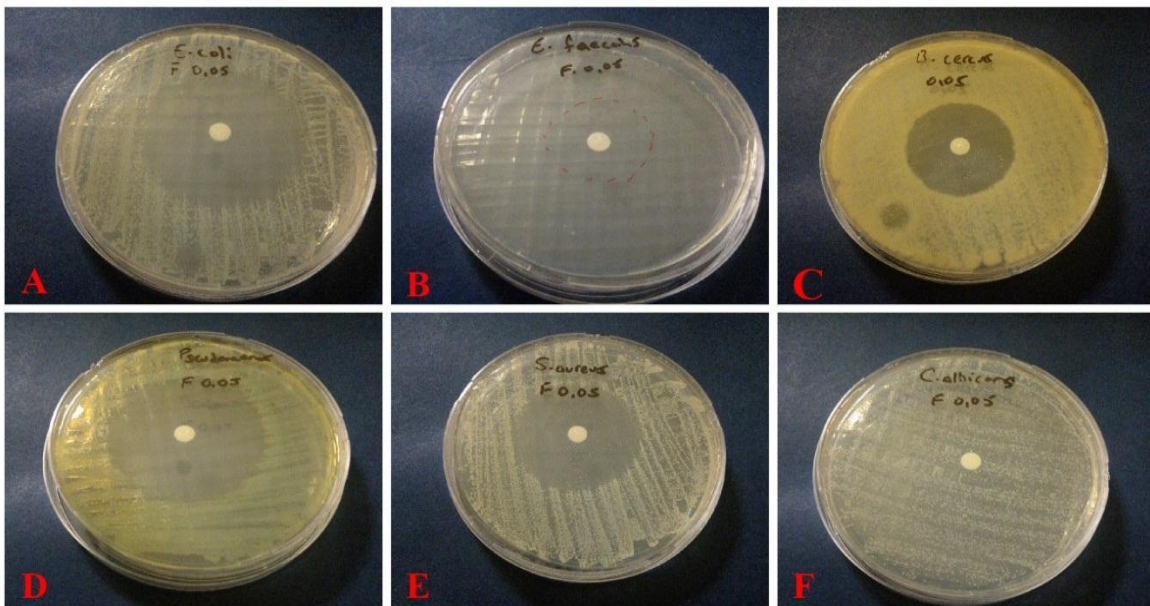


Figure 3.2.1: Shows the zone of inhibition for sample $F_{0.05}$

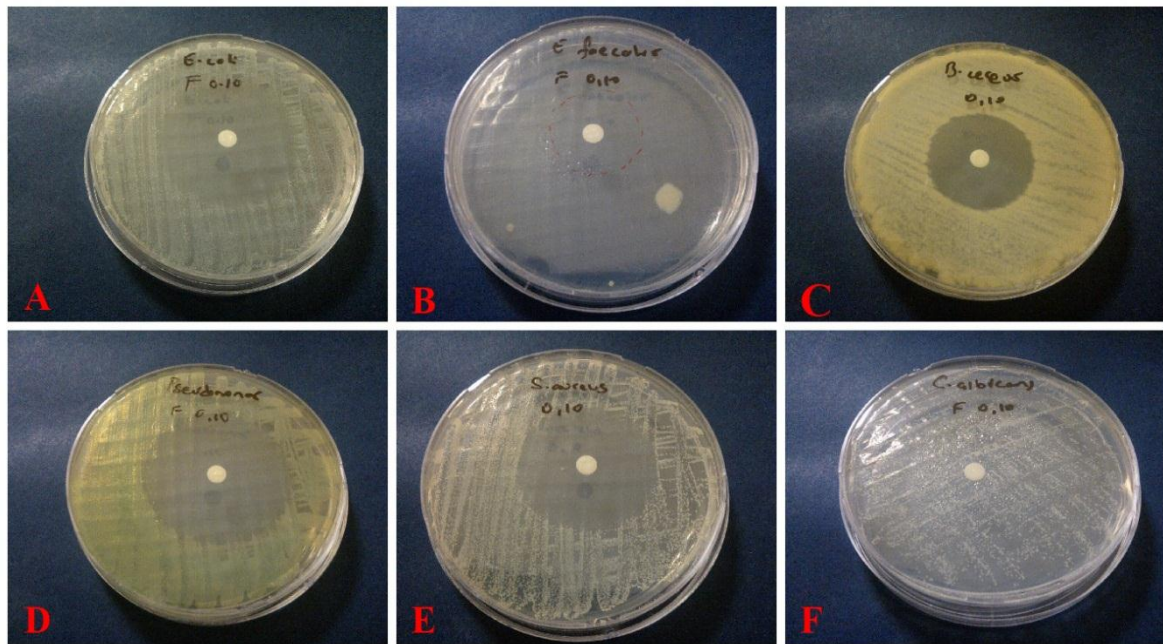


Figure 3.2.2: Shows the zone of inhibition for sample F_{0.10}

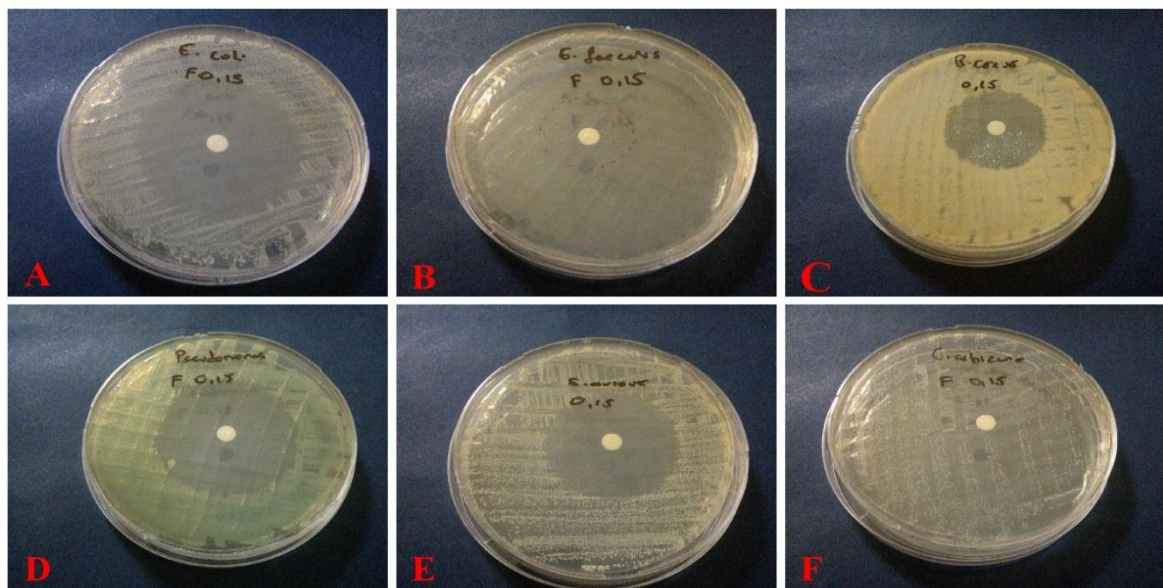


Figure 3.2.3: Shows the zone of inhibition for sample F_{0.15}

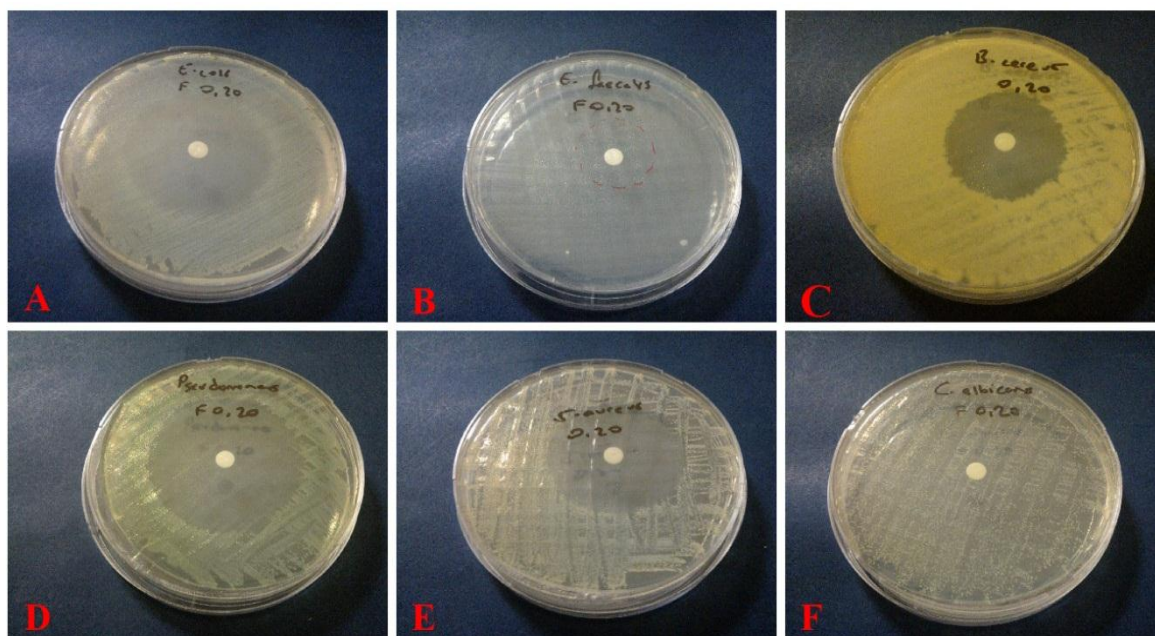


Figure 3.2.4: Shows the zone of inhibition for sample F_{0.20}

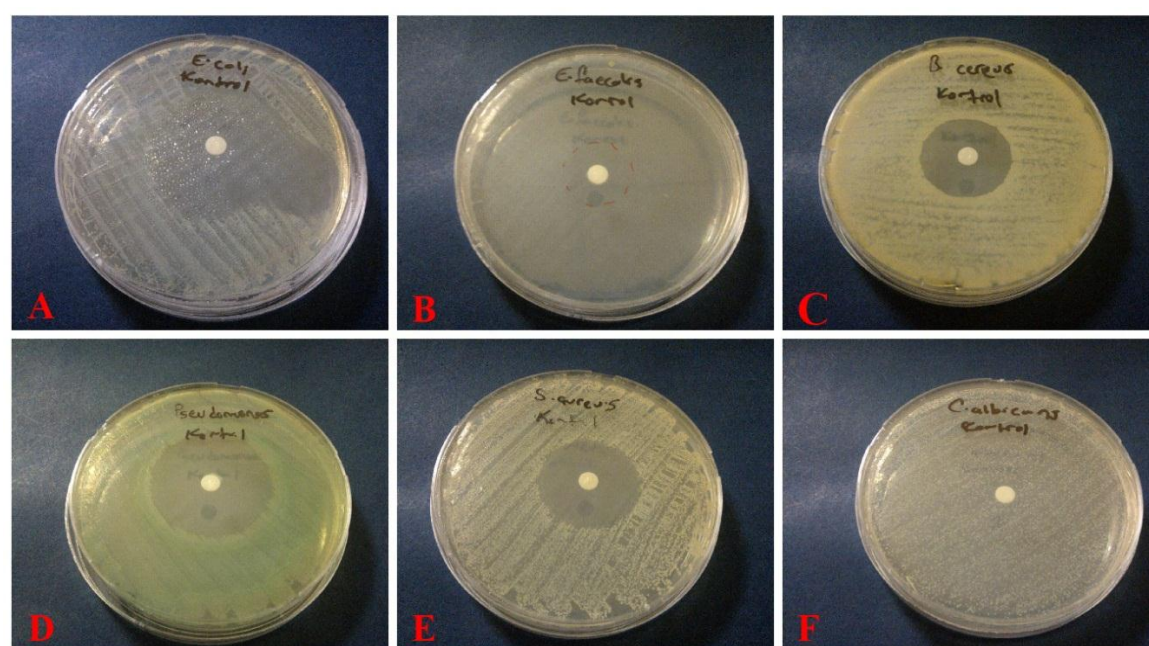


Figure 3.3.1: Shows the zone of inhibition for sample negative control which is SF MPs without drug.

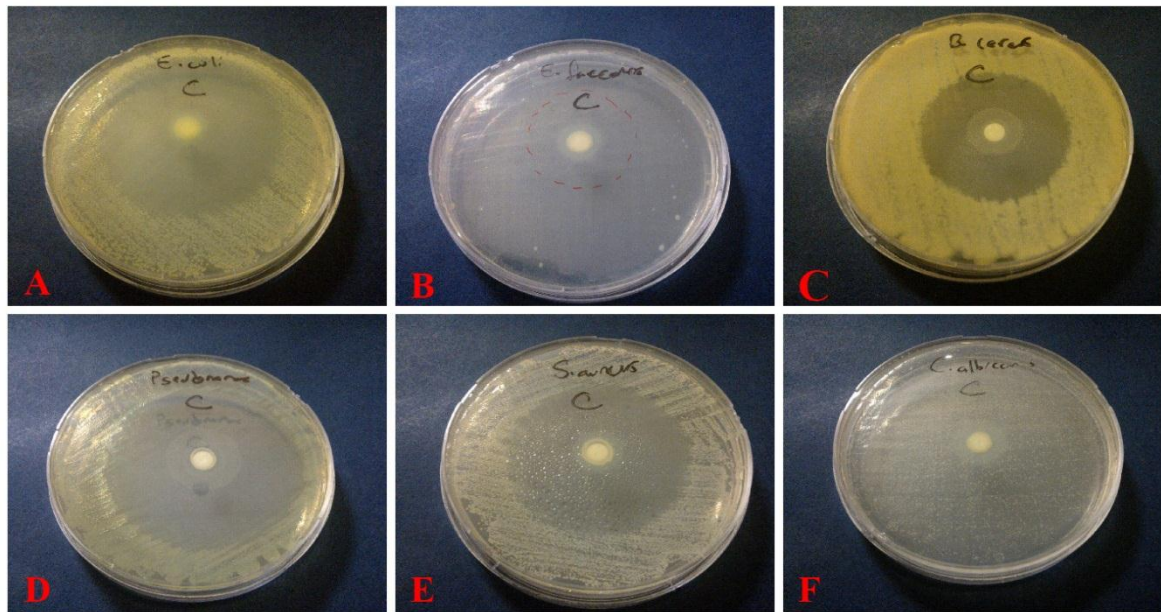


Figure 3.3.2: Shows the zone of inhibition of one of the positive control which is drug Cipro

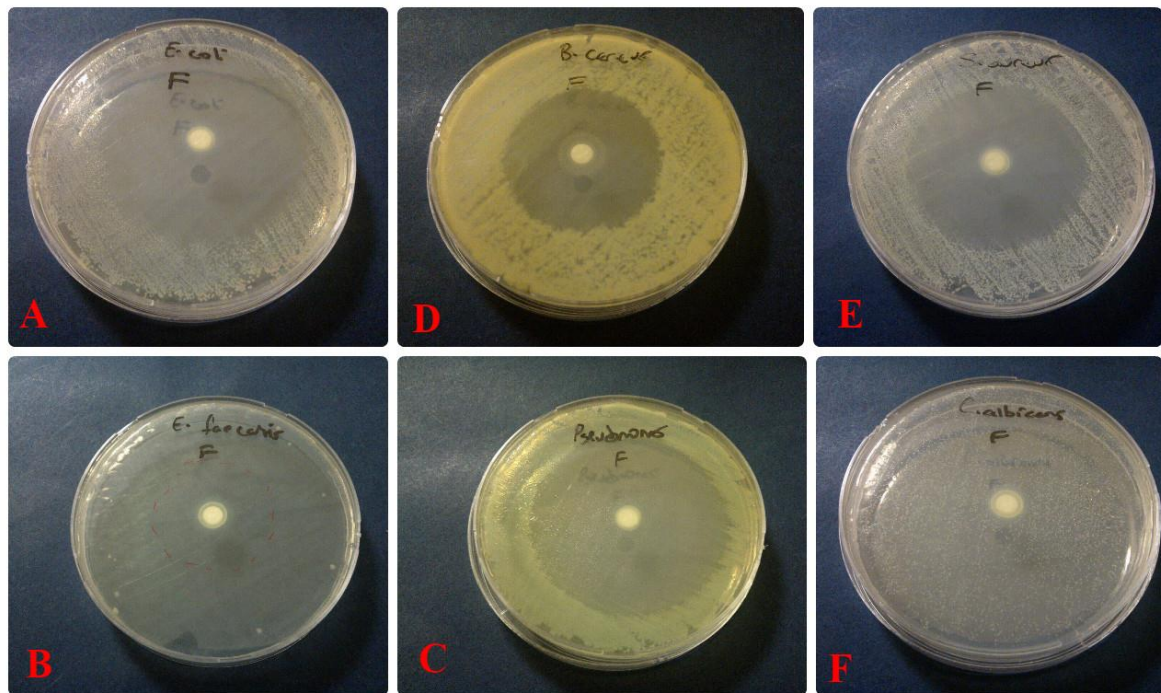


Figure 3.3.3: Shows the zone of inhibition of the other positive control which is drug Floxin

The figure above shows the antimicrobial action of different SF MPs loaded with Cipro and Floxin, along with the negative and positive control against *Escherichia coli*, *Bacillus cereus*, *Candida albicans* (no antimicrobial activity in all except in Cipro alone), *Staphylococcus aureus*, *Enterococcus faecalis* and *Pseudomonas aeruginosa* respectively.

Table 3.1: Showing the results of the antimicrobial susceptibility test supporting the above images or figure

Samples	<i>E.coli</i>	<i>E.faecalis</i>	<i>B.cereus</i>	<i>P.aeruginosa</i>	<i>S.aureus</i>	<i>C.albicans</i>
	(cm)	(cm)	(cm)	(cm)	(cm)	(cm)
C_{0.05}	4.0	3.3	3.7	4.4	4.5	-
C_{0.10}	3.9	3.0	3.3	4.5	3.5	-
C_{0.15}	3.8	2.9	3.2	4.6	3.8	-
C_{0.20}	4.5	3.1	3.4	4.7	3.8	-
F_{0.05}	4.6	2.9	3.2	4.5	4.0	-
F_{0.10}	4.5	2.8	3.4	4.6	3.9	-
F_{0.15}	4.7	2.7	3.5	4.7	4.0	-
F_{0.20}	4.4	2.5	3.6	4.8	4.2	-
Control	4.0	2.0	2.8	3.8	3.0	-
Cipro	6.0	3.6	4.4	5.9	5.2	1.4
Floxin	5.6	3.7	4.4	6.0	5.0	-

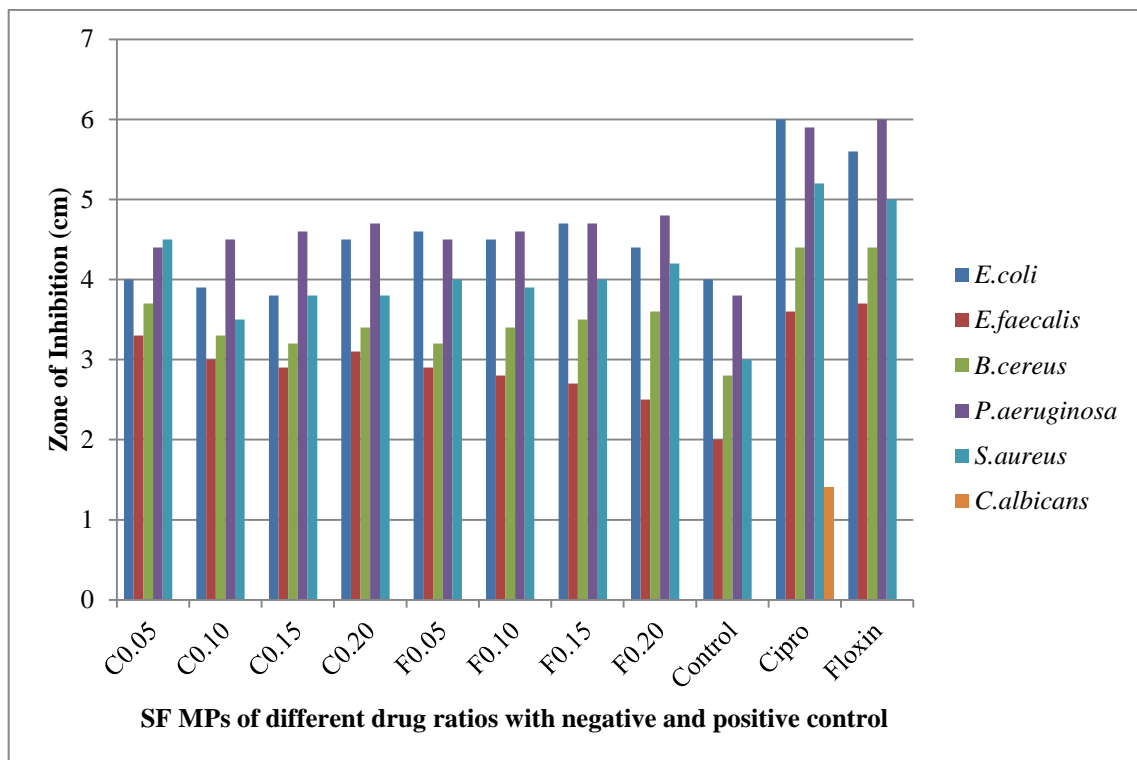


Figure 3.4: A bar graph presentation of antimicrobial activity

3.2.2 Scanning Electron Microscopy (SEM) analysis

SEM is a characterization technique that describes the size, structure and dispersion of the SF Microparticles loaded with drug. The figures below show the SEM micrograph of sample C_{0.20} at different μm and at different magnifications. Showing more of the morphology of the sample at numerous levels for better understanding of the structure.

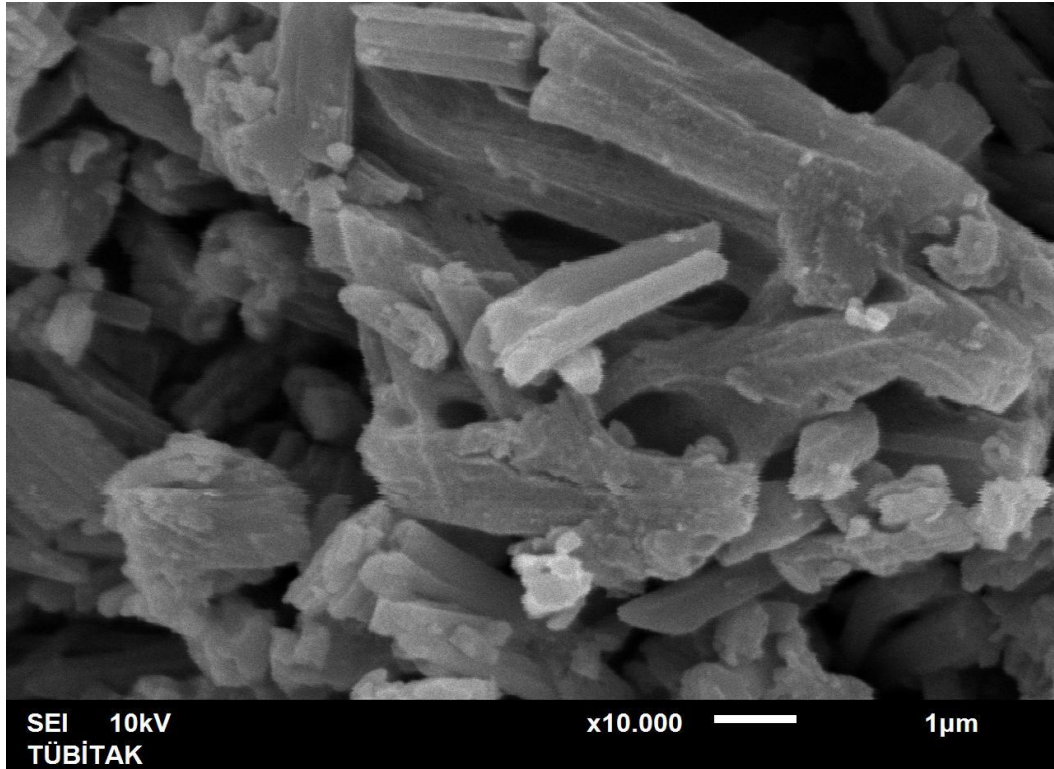


Figure 3.5.1: Shows SEM micrograph of sample C_{0.20} of 1µm at x10 magnification

The figure 3.5.1 above appears to be irregular having some rod-like and sphere-like structures. At this level, intricate details are seen at a magnification unlike the other images shown below, except for figure 3.5.6 which is very intricate in detailing.

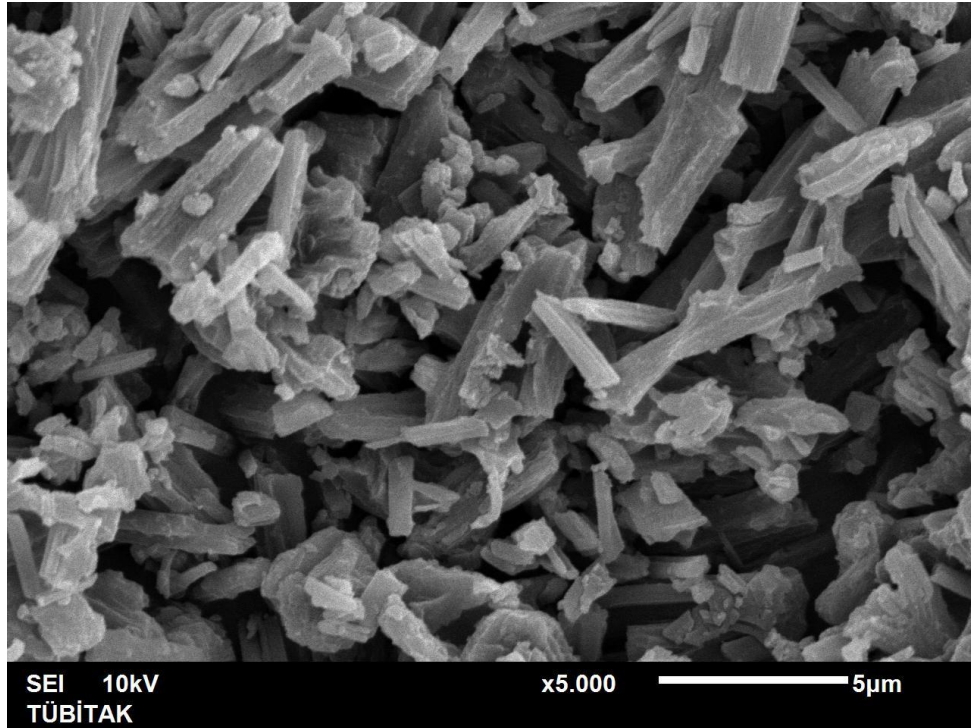


Figure 3.5.2: Shows SEM micrograph of sample $C_{0.20}$ of 5μm at x5 magnification

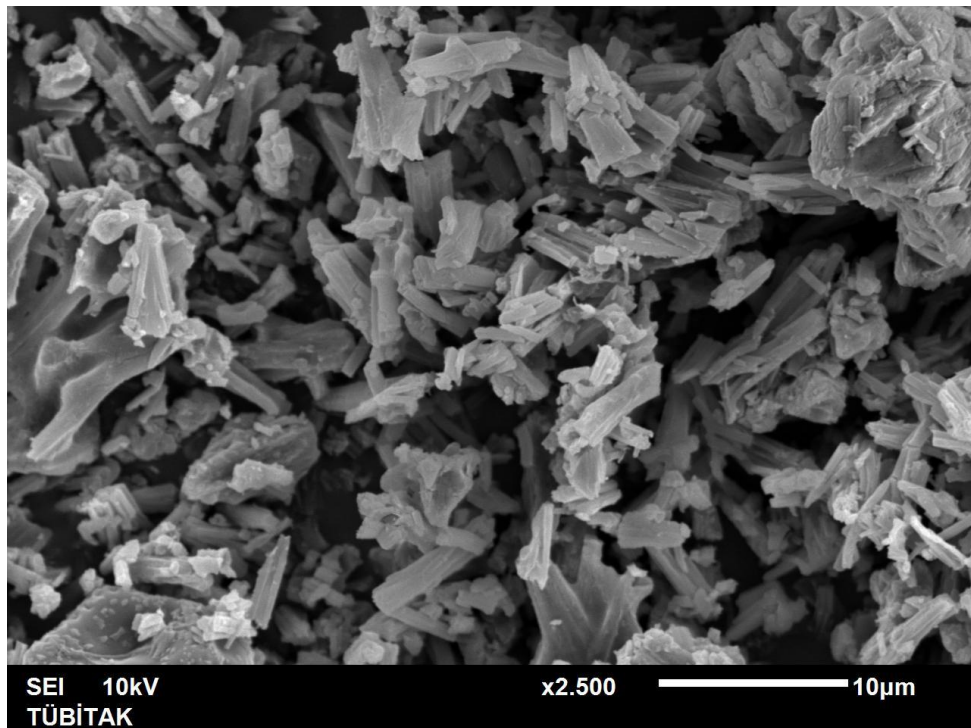


Figure 3.5.3: Shows SEM micrograph of sample $C_{0.20}$ of 10μm at x2.5 magnification

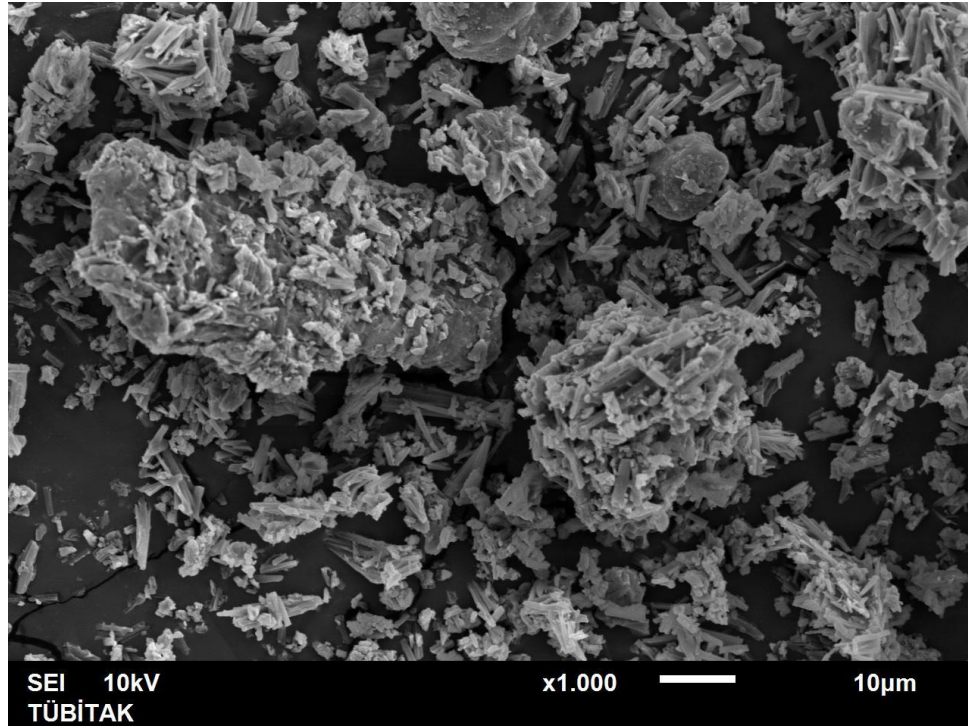


Figure 3.5.4: Shows SEM micrograph of sample C_{0.20} of 10µm at x1 magnification

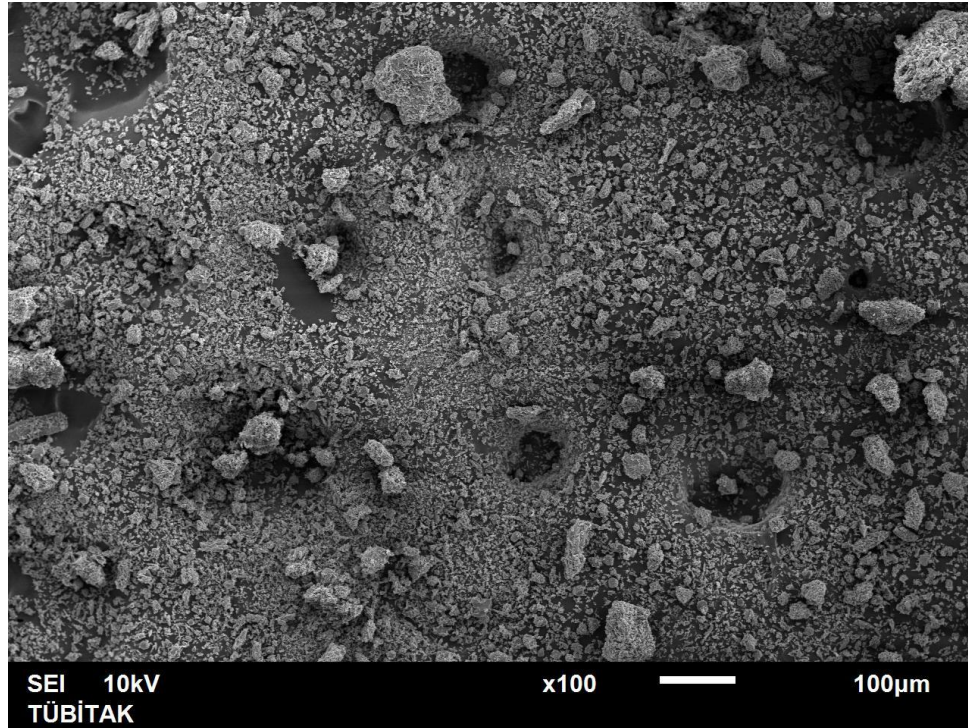


Figure 3.5.5: showing SEM micrograph of sample $C_{0.20}$ of 100µm at x100 magnification

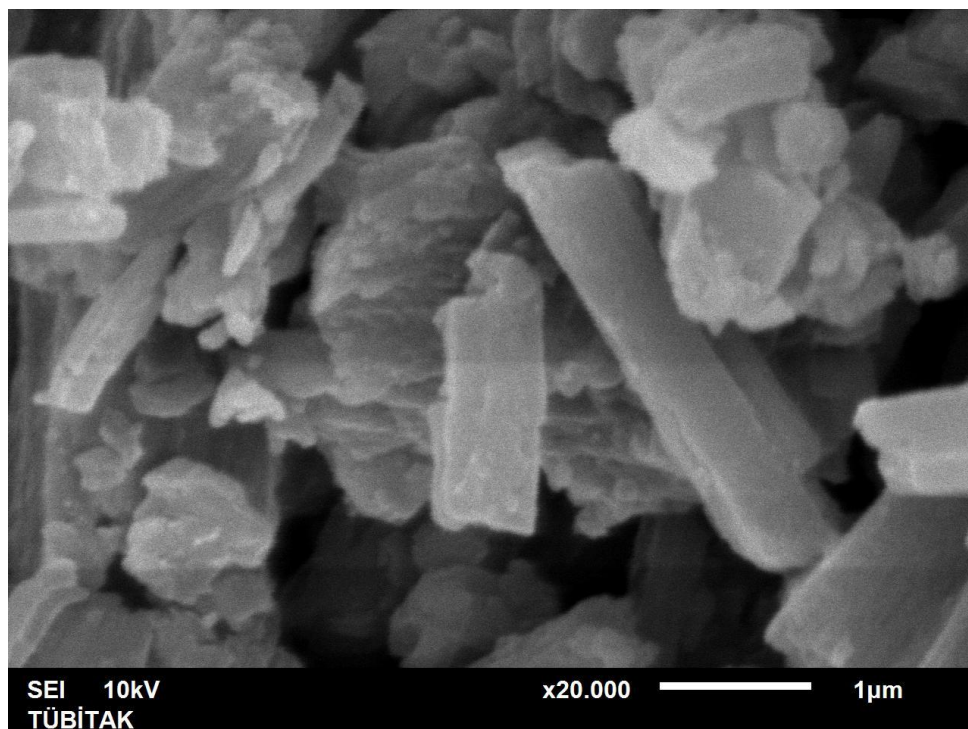


Figure 3.5.6: Showing SEM micrograph of sample $C_{0.20}$ of 1µm at x20 magnification

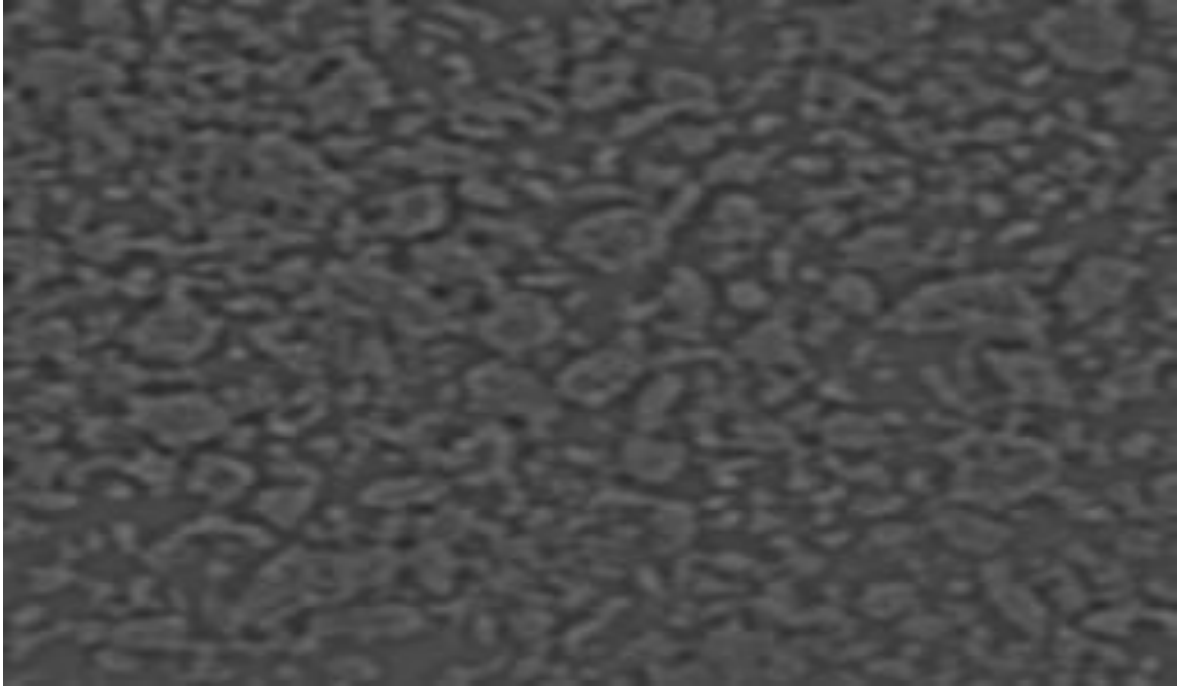


Figure 3.5.7: SEM micrograph duplicated from figure 3.5.5 and filtered for better analysis when using a software ImageJ to calculate particle diameter

Table 3.2: Showing the Excel sheet results of the analysed figure 3.5.7 using the ImageJ software and further processed in OriginLab software

	Area	Mean	Min	Max	r ²	r	d(μm)
1	64.556	103.226	95	112	20.54881	4.53308	9.06616
2	56.227	108.685	95	124	17.89761	4.230557	8.461113
3	29.155	102.857	95	116	9.280325	3.046363	6.092725
4	10.412	99.4	95	106	3.314243	1.820506	3.641012
5	3.124	96.667	96	98	0.9944	0.997196	1.994392
6	26.031	101.88	95	109	8.285925	2.878528	5.757056
7	78.092	107.84	95	128	24.85746	4.985725	9.97145
8	3.124	98.667	96	101	0.9944	0.997196	1.994392
9	19.783	99.789	95	105	6.297124	2.509407	5.018814
10	9.371	96.889	95	100	2.982882	1.727102	3.454204
11	84.34	104.988	95	123	26.84626	5.181337	10.36267
12	58.309	103.714	95	118	18.56033	4.30817	8.616341
13	77.051	106.392	95	122	24.5261	4.952383	9.904766
14	5.206	102.2	98	106	1.657121	1.287292	2.574584
15	73.928	103.803	95	117	23.53201	4.850981	9.701961
16	5.206	97.8	95	100	1.657121	1.287292	2.574584
17	31.237	101.567	95	109	9.943046	3.15326	6.306519
18	24.99	106.083	95	121	7.954564	2.820384	5.640767
19	62.474	100.75	95	110	19.88609	4.459382	8.918765
20	4.165	96.25	95	97	1.325761	1.151417	2.302834
21	36.443	103.714	95	116	11.60017	3.405902	6.811804
22	63.515	111.082	95	125	20.21745	4.496382	8.992764
23	21.866	101.619	95	109	6.960164	2.638212	5.276425

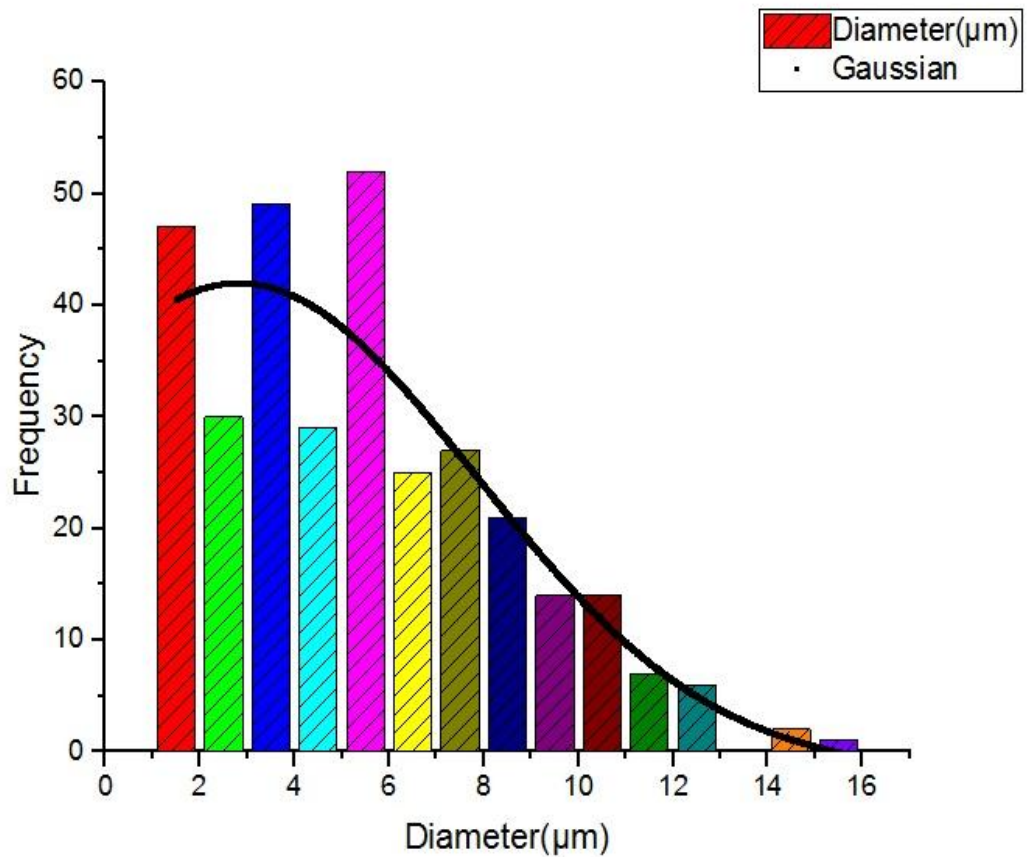


Figure 3.5.8: Gaussian plot showing the various diameters from the resized image in figure 3.5.7

Table 3.3: Showing the tabulated result of the Gaussian gotten from Software called OriginLab

Model	Gaussian		
Equation	$y = y_0 + A/(w \cdot \sqrt{\pi/(4 \cdot \ln(2))}) \cdot \exp(-4 \cdot \ln(2) \cdot (x - x_c)^2 / w^2)$		
Reduced Chi-Sqr	60.7136		
Adj. R-Square	0.80386		
		Value	Standard Error
Counts	y0	-1.76755	8.35131
Counts	xc	2.8057	1.65326
Counts	A	550.55171	313.65278
Counts	w	11.80672	4.77114

From the table 3.1 the average size of microparticle is indicated as 2.8057 μm and w indicates the standard deviation given as 11.80672 μm of the distribution of various diameters measured.

3.2.3 X-Ray Diffraction (XRD) Analysis

XRD is a technique used for determination and characterization of crystalline structure and purity of a sample. The use of XRD has been employed in experiments involving particles of different sizes especially in biosynthesis of micro and nanoparticles loaded with drug. The result of XRD presented below shows the peak intensity, the XRD provides two peak intensity of separate reflections and at small values of 2θ the peaks overlap each other. Thus, the result of the peak position is presented at 2θ and X-ray counts the intensity seen in the XY plot below. In Murphy and Romero (2014) the characteristic powder XRD peaks occur around 19.2° , 20.8° and 25.1° for beta-sheet and at 9.7° and 28.6° for random coil structures.

Also according to Kundu et al. (2010), Three types of crystalline structures are proposed for silk. The glandular state prior to crystallization is called the Silk I. Silk II is the spun silk state which consists of the β -sheet secondary structure and Silk III (an air/water assembled interfacial silk) is a helical structure (Kundu et al., 2008a,b). The main diffraction peaks of Silk I are present at around $2\theta = 12.2^\circ$ and 28.2° , while Silk II are present at about $2\theta = 18.9^\circ$ and 20.7° . About seven distinct peaks were found in the X-ray diffractograms in the regions between 5° and 35° . Sharp peaks at $2\theta = 8.68^\circ$ denoting the Silk I conformation and at $2\theta = 18.16^\circ$ denoting the Silk II structure appeared in the XRD pattern of the SF microparticles.

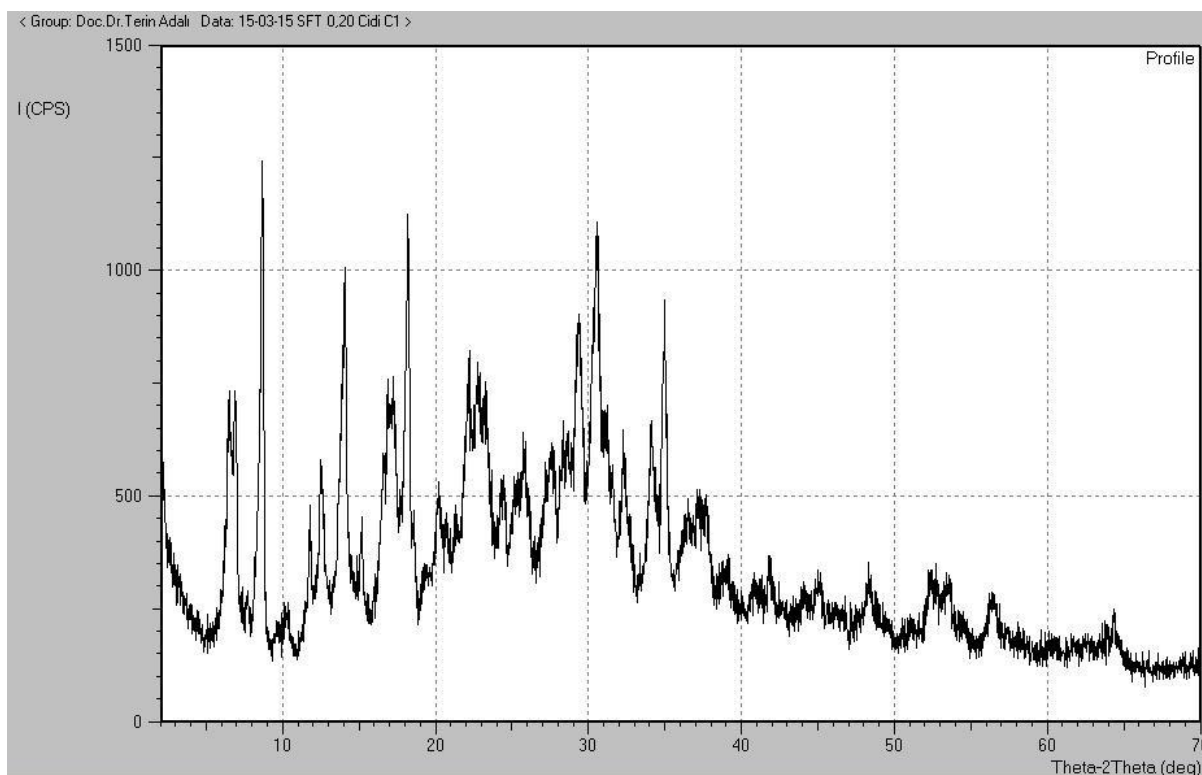


Figure 3.6: The XRD analysis result of the SF MPs loaded with Cipro showed that the degree of crystallinity and the crystalline structure were affected by the structural formation processes such that, the crosslinker helped in the formation ordered structure of silk fibroin MPs with the drug

3.3 Applications

The research can be potentially applied in drug delivery and wound healing. Most especially wound healing, the microparticles can effectively speed up wound drying process and also keeping the environment sterile. Diabetic patients might find a bit of relief from prolong healing of injury which results in serious infections that most often lead to amputation.

CHAPTER 4

CONCLUSION AND RECOMMENDATIONS

4.1 Conclusion

The result from this work affirms that silk fibroin has antibacterial properties, giving its other potent and numerous biomedical properties. The results establish further the importance of silk fibroin incorporated with potent drugs for enhanced delivery and resulting in excellent treatment. This research can also be greatly applied in wound healing for the effective drying and sterile condition of injury, diabetic patients might just have a possible solution to their extended wound healing process. Furthermore, the quest for an efficient drug delivery system might end with more standardized and heavily financed research on the subject.

4.2 Recommendations

Working with other biomaterials and drugs with unique properties; paving the way for giant breakthrough research in this field. The world of micro and nanoparticles flooded with numerous excellent biomaterials that will shake the fabric of biomedical engineering providing effective health care to individuals in need.

REFERENCES

- Altman, G., Diaz, F., Jakuba, C., Calabro, T., Horan, R., Chen, J., & Kaplan, D. (2003). Silk-based biomaterials. *Biomaterials*, 24(3), 401–16.
- Aramwit, P. (2014). Bio-response to silk sericin, in silk biomaterials for tissue engineering and regenerative medicine. edited by S.C. Kundu, (pp. 299-329). Sawston, Cambridge: Woodhead Publishing.
- Aramwit, P., Siritientong, T., & Srichana, T. (2012). Potential applications of silk sericin, a natural protein from textile industry by-products. *Waste Management Resources*, 30, 217–24.
- Ayutsede, J., Gandhi, M., Sukigara, S., Micklus, M., Chen, H.E., & Ko, F. (2005). Regeneration of Bombyx mori silk by electrospinning. Part 3: characterization of electrospun non-woven mat. *Polymer*, 46(5), 1625-1634.
- Bailey, K. (2013). Potential Applications of Silk Fibroin as a Biomaterial. Retrieved August 6, 2015 from https://uwspace.uwaterloo.ca/bitstream/handle/10012/7621/Bailey_Kevin.pdf?sequence=1
- Brill, R. (1943). Relations between the structures of poly-amides and silk fibers (in German). *Zeitschrift für Physikalische Chemie*, 53 , 61-74.
- Chirila, T., Suzuki, S., Bray, L., Barnett, N., & Harkin, D. (2013) Evaluation of silk sericin as a biomaterial: in vitro growth of human corneal limbal epithelial cells on Bombyx mori sericin membranes, *Progress in Biomaterials* 2, 122-145.
- Chung, T.W., Chang, C.H., & Ho, C.W. (2011). Incorporating Chitosan (CS) and TPP into silk fibroin (SF) in fabricating spray-dried microparticles prolongs the release of a hydrophilic drug. *Journal of the Taiwan Institute of Chemical Engineers*, 42(4), 592-597.

- Clinical and Laboratory Standards Institute (CLSI) (2012). Performance Standards for Antimicrobial Disk Susceptibility Tests; Approved Standard—Eleventh Edition. CLSI document M02-A11. 17th informational supplement M100- S22. Wayne, Pennsylvania: Technology and Society Magazine.
- Hazeri, N., Tavanai, H., & Moradi, A. R. (2012). Production and properties of electrosprayed sericin nanopowder. *Science and Technology of Advanced Materials*, 13(3), 1-7.
- Herzog, R.O., & Jancke, W. (1920). Ü ber den physikalischen Aufbau einiger hochmolekularer organischer Verbindungen. (1. vorlä ufi ge Mitteilung.). *Berichte der Deutschen Chemischen Gesellschaft*, 53 , 2162-2164.
- Hu, X., & Kaplan, D. L. (2011). Silk Biomaterials. *Comprehensive Biomaterials*, 207-219.
- Jasmine S., & Mandal B.B. (2014). Types and properties of non-mulberry silk biomaterials for tissue engineering applications, In *Silk Biomaterials for Tissue Engineering and Regenerative Medicine*, edited by S.C. Kundu, (pp. 275-298), Sawston, Cambridge: Woodhead Publishing.
- Koh, L.D., Cheng, Y., Teng, C.P., Khin, Y.W., Loh, X.J., Tee, S.Y., & Han, M.Y. (2015). Structures, mechanical properties and applications of silk fibroin materials. *Progress in Polymer Science*, 46, 86-110.
- Kundu, J., Chung, Y.I., Kim, Y., Tae, G., & Kundu, S. (2010). Silk fibroin nanoparticles for cellular uptake and control release. *International Journal of Pharmaceutics*, 388(2), 242-250.
- Kundu, J., Dewan, M., Ghoshal, S., & Kundu, S.C. (2008a). Mulberry non-engineered silk gland protein vis-à-vis silk cocoon protein engineered by silkworms as biomaterial matrices. *Journal of Material Science: Materials in Medicine*, 19, 2679–2689.

- Kundu, J., Patra, C., & Kundu, S.C. (2008b). Design, fabrication and characterization of silk fibroin-HPMC-PEG blended films as vehicle for transmucosal delivery. *Material Science Engineering: C*, 28, 1376–1380.
- Kunjachan, S., & Jose, S. (2010). Understanding the mechanism of ionic gelation for synthesis of chitosan nanoparticles using qualitative techniques. *Asian Journal of Pharmaceutics*, 4(2), 148.
- Mahendran, B., Ghosh, S. K., & Kundu, S. C. (2006). Molecular phylogeny of silk-producing insects based on internal transcribed spacer DNA1. *Journal of Biochemistry and Molecular Biology*, 39(5), 522–529.
- Marsh, R.E., Corey, R.B. & Pauling, L. (1955). An investigation of the structure of silk fibroin. *Biochimica et Biophysica Acta*, 16(1), 1–34.
- Meinel, L., Hofmann, S., Karageorgiou, V., Kirker-Head, C., McCool, J., & Gronowicz, G. (2005). The Inflammatory Responses to Silk Films in Vitro and in Vivo. *Biomaterials*, 26, 147.
- Murphy, A.R. & Romero I.S. (2014). Biochemical and biophysical properties of native Bombyx mori silk for tissue engineering applications, In *Silk Biomaterials for Tissue Engineering and Regenerative Medicine*, edited by S.C. Kundu, (pp. 219-238), Sawston, Cambridge: Woodhead Publishing.
- Lawrence, B.D. (2014). Processing of Bombyx mori silk for biomedical applications, In *Silk Biomaterials for Tissue Engineering and Regenerative Medicine*, edited by Kundu S.C., (pp. 78-99), Sawston, Cambridge: Woodhead Publishing.
- Liu, H., Ge, Z., Wang, Y., Toh, S. L., Sutthikhum, V., & Goh, J. C. (2007). Modification of sericin-free silk fibers for ligament tissue engineering application. *Journal of Biomedical Materials Research Part B: Applied Biomaterials*, 82(1), 129-138.
- Li, X., Zhang, L., Wang, Y., Yang, X., Zhao, N., Zhang, X., & Xu, J. (2011). A bottom-up approach to fabricate patterned surfaces with asymmetrical TiO₂

- microparticles trapped in the holes of honeycombl like polymer film. *Journal of the American Chemical Society*, 133(11), 3736–3739.
- Okazaki, Y., Tomotake, H., Tsujimoto, K., Sasaki, M., & Kato, N. (2011). Consumption of a resistant protein, sericin, elevates fecal immunoglobulin A, mucins, and cecal organic acids in rats fed a high-fat diet. *The Journal of nutrition*, 141(11), 1975-1981.
- Patil, P, Chavanke, D, & Wagh, M. (2012). A review on ionotropic gelation method: novel approach for controlled gastroretentive gelispheres. *International Journal of Pharmacy and Pharmceutical Science*, 4, 27-32
- Pérez-Rigueiro, J., Elices, M., Llorca, J., & Viney, C. (2001). Tensile properties of silkworm silk obtained by forced silking. *Journal of Applied Polymer Science*, 82(8), 1928-1935.
- Prasad, M.D., Muthulakshmi, M., Arunkumar, K.P., Madhu, M., Sreenu, V.B., Pavithra, V., Bose, B., Nagarajaram, H.A., Mita, K., Shimada, T., & Nagaraju, J. (2005). SilkSatDb: A microsatellite database of the silkworm, Bombyx mori. *Nucleic Acids Research*, 33, 403-406
- Pritchard, E. M., & Kaplan, D. L. (2011). Silk fibroin biomaterials for controlled release drug delivery. *Expert opinion on drug delivery*, 8(6), 797-811.
- Rajkhowa, R., & Wang, X. (2014). Silk powder for regenerative medicine, In *Silk Biomaterials for Tissue Engineering and Regenerative Medicine*, edited by S.C. Kundu, (pp. 191-216), Sawston, Cambridge: Woodhead Publishing.
- Sionkowska, A. (2011). Current Research on the Blends of Natural and Synthetic Polymers as New Biomaterials. *Progress in Polymer Science*, 1254-1276.
- Talukdar, S., & Kundu, S.C. (2014). Silk scaffolds for three-dimensional (3D) tumor modeling, In *Silk Biomaterials for Tissue Engineering and Regenerative Medicine*, edited by S.C. Kundu, (pp. 472-502), Sawston, Cambridge: Woodhead Publishing.

- Thirupathamma, D., Savithri, G., & Kavya, S.K. (2013). Silk for biomedical applications. *Research Journal of Pharmaceutical, Biological and Chemical Sciences*, 4(2), 657
- Vert, M., Li, S.M., Spenlehauer, G., & Guerin, P. (1992). Bioresorbability and biocompatibility of aliphatic polyesters, *Journal of Material Science: Materials in Medicine*, 3, 432–446.
- Wang, Y., Rudym, D.D., Walsh, A., Abrahamsen, L., Kim, H.J., Kim, H.S., Kirker-Head, C., & Kaplan, D.L. (2008). *In vivo* degradation of three-dimensional silk fibroin scaffolds. *Biomaterials*, 29, 3415–3428.
- Wenk, E., Merkle, H., & Meinel, L. (2010). Silk fibroin as a vehicle for drug delivery applications. *Journal of controlled release : official journal of the Controlled Release Society*, 150(2), 128–141
- Williams, D.F. (1999). The Williams Dictionary of Biomaterials. Liverpool, United Kingdom: Liverpool University Press.
- Winsted Silk Co. (1915). The Silkworm: its history and product, Illinois, Chicago: Library of Congress.
- Zhang, P., & Guan, J. (2011). Fabrication of Multilayered Microparticles by Integrating Layer-by-Layer Assembly and MicroContact Printing. *Small*, 7(21), 2998–3004.